Hydrochemical tracers in the middle Rio Grande Basin, USA: 1. Conceptualization of groundwater flow

L. Niel Plummer · Laura M. Bexfield · Scott K. Anderholm · Ward E. Sanford · Eurybiades Busenberg

Abstract Chemical and isotopic data for groundwater from throughout the Middle Rio Grande Basin, central New Mexico, USA, were used to identify and map groundwater flow from 12 sources of water to the basin, evaluate radiocarbon ages, and refine the conceptual model of the Santa Fe Group aquifer system.

Hydrochemical zones, representing groundwater flow over thousands to tens of thousands of years, can be traced over large distances through the primarily siliciclastic aquifer system. The locations of the hydrochemical zones mostly reflect the "modern" predevelopment hydraulic-head distribution, but are inconsistent with a trough in predevelopment water levels in the west-central part of the basin, indicating that this trough is a transient rather than a long-term feature of the aquifer system. Radiocarbon ages adjusted for geochemical reactions, mixing, and evapotranspiration/dilution processes in the aquifer system were nearly identical to the unadjusted radiocarbon ages, and ranged from modern to more than 30 ka. Age gradients from piezometer nests ranged from 0.1 to 2 year cm^{-1} and indicate a recharge rate of about 3 cm $year^{-1}$ for recharge along the eastern mountain front and infiltration from the Rio Grande near Albuquerque. There has been appreciably less recharge along the eastern mountain front north and south of Albuquerque.

Résumé Des données sur les éléments chimiques et les isotopes présents dans l'eau souterraine prélevée à divers endroits dans le bassin moyen du Rio Grande, au centre du Nouveau-Mexique (É-U), ont permis de déterminer l'existence et l'étendue de douze sources d'eau régionales dans le bassin, d'évaluer les âges radiocarbones et de raffiner le modèle conceptuel du système aquifère du groupe de Santa Fe. Des zones hydro-chimiques qui représentent l'écoulement de l'eau souterraine depuis des dizaines de milliers d'années peuvent être suivies sur de longues distances à travers l'aquifère principalement siliclastique. La position des zones hydro-chimiques reflète principalement la distribution moderne des charges hydrauliques mais est incohérente avec une dépression dans le niveau d'eau dans la partie centre-ouest du bassin, ce qui indique que cette dépression est un élément transitoire du système aquifère plutôt qu'un élément à long terme. Les âges radiocarbones ajustés aux réactions géochimiques et aux processus de mélange et d'évapotranspiration/dilution qui ont lieu dans l'aquifère sont presque identiques aux âges non ajustés et varient de la période moderne jusqu'à 30 ka. Les gradients d'âge établis à partir des nids de piézomètres s'étendent de 0.1 à 2 a cm^{-1} et suggèrent un taux de recharge d'environ 3 cm a^{-1} le long du front des montagnes à l'est et pour l'infiltration provenant du Rio Grande près d'Albuquerque. Il y a eu substantiellement moins de recharge le long du front des montagnes à l'est, au nord et au sud d'Albuquerque.

Resumen Se utilizaron datos químicos e isotópicos de agua subterránea a lo largo de la cuenca central del río Grande, Nuevo México, EEUU, para identificar y mapear el flujo de agua subterránea de 12 fuentes de agua a la cuenca para evaluar edades por medio de radio carbon y para refinar el modelo conceptual del sistema acuífero del Grupo Santa Fé.

Se puede establecer zonas hidrotérmicas que representan el flujo de agua subterránea a lo largo de miles a miles de decenas de años en grandes distancias a través del sistema acuífero principalmente siliclástico. Las ubicaciones de las zonas hidroquímicas mayormente reflejan la distribucion de la cabeza hidráulica pre-desarollo moderna pero son inconsistentes con una depresión en los niveles de agua pre-desarollo en la zona central oeste de la cuenca. Esto indica que esta depresión es un rasgo transitorio y no un rasgo de largo plazo del sistema acuífero. Las edades de radio carbon ajustadas para los procesos de reaciones geoquímicas, de mezclado y de evapotranspiración-dilución son casi idénticas a los edades de radio carbon no ajustadas oscilan en un rango desde la modernidad a 30 mil años. Las gradientes de edad de nidos de piezometros van de 0.1 a 2 años cm^{-1} e indican un sitio de recarga de aproximadamente 3 cm/yr

Received: 29 November 2002 / Accepted: 7 January 2004
Published online: 25 May 2004

© Springer-Verlag 2004

L. N. Plummer (✉) · W. E. Sanford · E. Busenberg
US Geological Survey,
432 National Center, Reston, VA 20192, USA
e-mail: nplummer@usgs.gov

L. M. Bexfield · S. K. Anderholm
US Geological Survey,
5338 Montgomery, NE, Suite 400, Albuquerque, NM 87109, USA

 DOI 10.1007/s10040-004-0324-6

para la recarga a lo largo del frente montañoso oriental e infiltración del río Grande cerca de Albuquerque. Se aprecia una recarga menor a lo largo del frente oriental de montañas al norte y al sur de Albuquerque.

Keywords Arid regions · Hydrochemistry · New Mexico · Radiocarbon age · Stable isotopes

Introduction

Since the mid-1940s, groundwater withdrawals in the vicinity of Albuquerque, New Mexico (Fig. 1), have resulted in declines in water levels in excess of 36 m (Bexfield and Anderholm 2002). Hawley and Haase (1992) showed that the highly productive sediments of the Santa Fe Group aquifer system, from which the city of Albuquerque obtains its water supply, are much less ex-

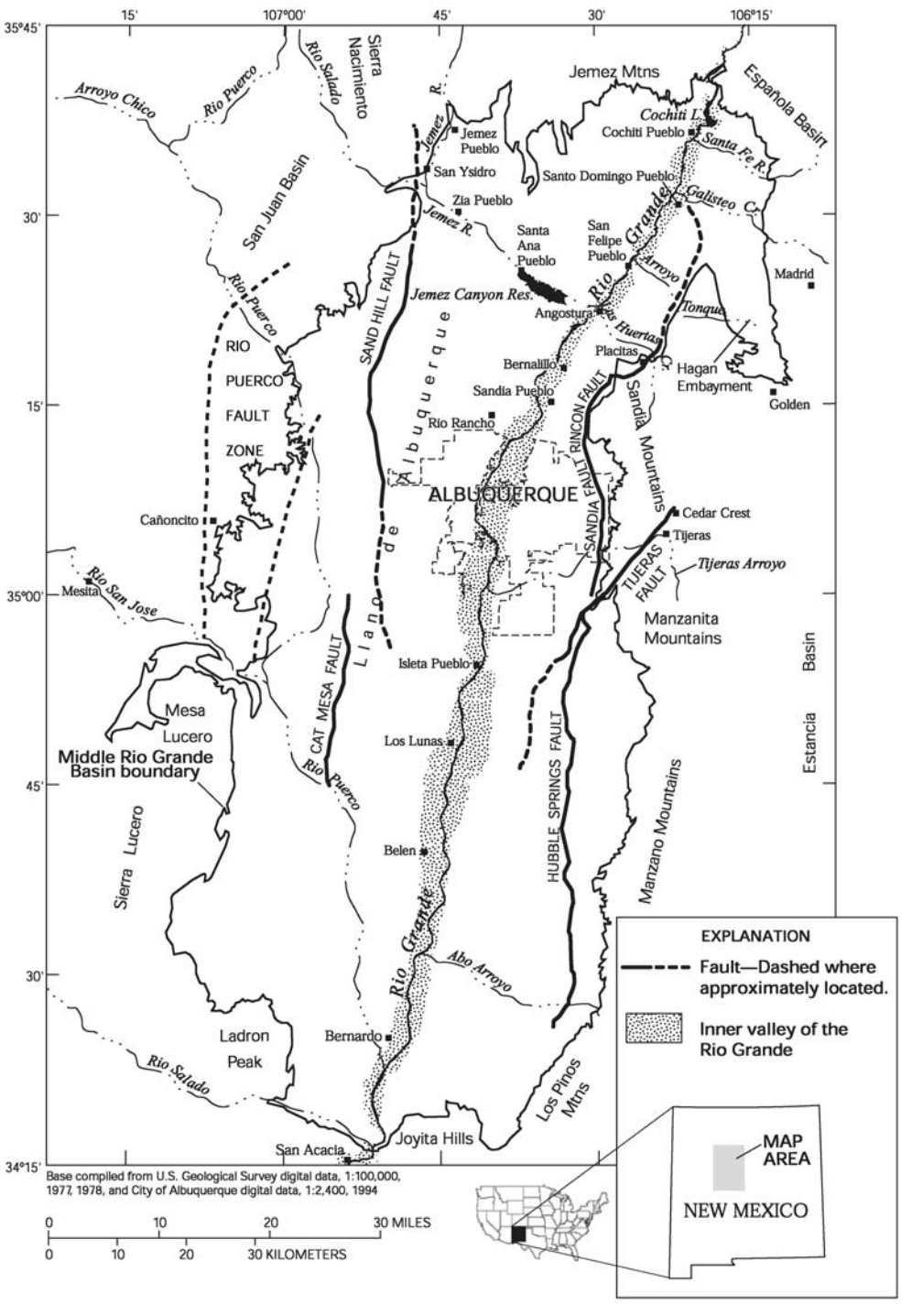

Fig. 1 Selected features of the Middle Rio Grande Basin

 DOI 10.1007/s10040-004-0324-6

tensive and thinner than previously thought (Bjorklund and Maxwell 1961; Reeder et al. 1967). A series of investigations was conducted beginning in the early 1990s to improve understanding of the geohydrologic framework and hydrologic conditions in the aquifer system (Hawley and Haase 1992; Thorn et al. 1993; Hawley et al. 1995; Kernodle et al. 1995; Thomas 1995; Constantz and Thomas 1996; Haneberg and Hawley 1996; Hawley 1996a; McAda 1996; Anderholm 1997; Bexfield and Anderholm 1997, 2000, 2002; Connell et al. 1998; Stone et al. 1998; Tiedeman et al. 1998; Grauch et al. 1999, 2001; Bartolino and Niswonger 1999; Bexfield et al. 1999; Anderholm 2001; Connell 2001; Sanford et al. 2001; Bartolino and Cole 2002; McAda and Barroll 2002; Plummer et al. 2004; Sanford et al. 2004a, 2004b), and to incorporate the new information into improved versions of groundwater-flow models for the basin (Kernodle et al. 1987, 1995; Kernodle 1998; McAda and Barroll 2002; Sanford et al. 2004a, 2004b). Much of the recent hydrogeologic and geochemical work in the Middle Rio Grande Basin (MRGB) was conducted by the US Geological Survey (US Geol Surv), in cooperation with other Federal, State, and local agencies, as part of a 6-year (1995–2001) investigation of the geology and hydrology of the MRGB (Bartolino and Cole 2002). This paper presents results from one part of the overall US Geol Surv investigation, in which chemical and isotopic data from groundwater in the MRGB were used to identify and map groundwater flow of various sources of water to the basin, evaluate radiocarbon ages, and refine the conceptual model of the Santa Fe Group aquifer system. These data are subsequently used to provide input to a groundwater-flow model (Sanford et al. 2004a, 2004b).

The data set collected for this study (Plummer et al. 2004) is uniquely large and comprehensive. A wide variety of constituents, including 30 major and minor elements, were sampled at 288 wells and springs. Other constituents included stable isotopes of water (^{2}H and ^{18}O), stable carbon isotopic composition (^{13}C) of dissolved inorganic carbon (DIC), stable sulfur isotopic composition (^{34}S) of dissolved sulfate (SO_4), radioactive carbon isotopic composition (^{14}C) of DIC, concentrations of dissolved nitrogen (N_2), argon (Ar), helium (He), neon (Ne), sulfur hexafluoride (SF_6), chlorofluorocarbons (CFCs), tritium (^{3}H), and tritiogenic helium-3 ($^{3}He_{tri}$) in groundwater. All of the chemical and isotopic data are given in Plummer et al. (2004), where additional data on the chemical and isotopic composition of surface water also are tabulated.

This study demonstrates some of the benefits of obtaining a diverse and extensive chemical and isotopic dataset when characterizing hydrochemical processes in groundwater systems and/or refining a conceptual model of the groundwater-flow system. In the companion paper (Sanford et al. 2004b), the radiocarbon ages and conceptualization of groundwater flow from this investigation are used in conjunction with other hydrogeologic data to refine a groundwater-flow model for the basin.

Description of the Study Area

The MRGB covers about 7,900 km^2 (Fig. 1) and contains basin-fill deposits up to about 4.2 km thick (Thorn et al. 1993) in the Rio Grande rift of central New Mexico. The basin is partly surrounded by mountain ranges, which include the Jemez Mountains to the north; the Sandia, Manzanita, Manzano, and Los Pinos Mountains to the east; and the Joyita Hills and Ladron Peak to the south (Fig. 1). The west side of the basin is bounded by the Lucero and Nacimiento uplifts and the Rio Puerco fault zone.

The climate of the MRGB is semiarid, although parts of the surrounding mountainous areas are humid continental (Thorn et al. 1993). Mean annual precipitation at Albuquerque (altitude 1,618 m) averaged 21.8 cm between 1914–2003, and 48.3 cm at Sandia Park (altitude 2,139 m) in the Sandia Mountains above Albuquerque. For the same period of record, mean annual snowfall averaged 25.1 cm at Albuquerque and 149 cm at Sandia Park.

The main surface drainage for the MRGB is the Rio Grande, which extends the entire length of the basin (Fig. 1), with headwaters in the San Juan Mountains of southwestern Colorado. The Rio Grande alternately gains and loses as it flows through the MRGB. At the north end of the basin, groundwater inflow apparently adds to discharge in the river between Cochiti Dam and San Felipe. Several tributaries, including the Jemez River and Rio Puerco, contribute substantial flow to the Rio Grande, and, potentially, can contribute substantial quantities of recharge to the underlying aquifer system. Numerous arroyos and ephemeral channels also can carry substantial quantities of water to the Rio Grande during large storm events and provide additional recharge to the aquifer system. Other sources of water to the basin include mountain-front recharge, direct infiltration of precipitation to basin-fill deposits, infiltration of runoff in arroyos that have headwaters in the alluvial basin, infiltration of water from perennial streams that cross the alluvial basin (Anderholm 2001), and subsurface inflow from adjacent basins. Mountain-front recharge includes infiltration of flow from streams that have headwaters in the mountainous area adjacent to the basin, and groundwater inflow from the mountainous area (Anderholm 2001).

For background on the geologic setting of the MRGB, the reader is referred to Kelley (1977), Lozinsky (1988), Anderholm (1988), Russell and Snelson (1990), Heywood (1992), Hawley and Haase (1992), Thorn et al. (1993), Haneberg and Hawley (1996), Minor and Shock (1998), Grauch et al. (1999, 2001), and Connell (2001).

Santa Fe Group Aquifer System

The primary aquifer of the MRGB consists of the unconsolidated to moderately consolidated basin-fill sediments of the Santa Fe Group. The Santa Fe Group aquifer system includes the Oligocene to middle Pleistocene Santa Fe Group deposits, and the more recent flood-plain,

 DOI 10.1007/s10040-004-0324-6

channel, and basin-fill deposits of Pleistocene to Holocene age that are in hydraulic connection with the Santa Fe Group deposits (Thorn et al. 1993). Hawley and Haase (1992) provide a detailed discussion of the hydrostratigraphic and lithofacies units of the aquifer system in the vicinity of Albuquerque, where the largest body of information is available.

Petrographic studies indicate a mineralogy consisting primarily of quartz, feldspar, and rock fragments, with lesser amounts of biotite, muscovite, chlorite, and heavy minerals (Hawley and Haase 1992). Rock fragments are volcanic, granitic/gneissic, sedimentary, and metamorphic, with volcanic fragments most abundant. Fine-grained sediments consist primarily of clay, with lesser amounts of sand and silt, and occasional calcite cement. The principal clay minerals are smectite, illite, kaolinite, and interlayered illite/smectite. The bulk composition of well cuttings was estimated to be approximately 60% granitic–metamorphic detritus of Precambrian derivation, 30% volcanic detritus of middle Tertiary derivation, and less than 10% sedimentary detritus of Paleozoic or Mesozoic derivation (Hawley and Haase 1992). Additional petrographic data are given by Lozinsky (1988), Stone et al. (1998), and Anderholm (1985).

Cementation is primarily by calcite and affects the hydraulic conductivity of aquifer materials across parts of the basin. Calcite has been observed in Quaternary deposits, such as those capping the mesa that separates the valleys of the Rio Grande and Rio Puerco (Kelley 1977). Below the northeastern part of Albuquerque, Hawley and Haase (1992) observed that Santa Fe Group sediments were mostly unconsolidated or poorly cemented to a depth of about 400 m. However, they did find caliche-cemented sandstones in about the upper 60 m of strata. Cementation and induration were observed to be significant at depths of ~500–600 m. Calcite has also been noted as the primary cement in other parts of the basin (Lozinsky 1988; Mozley and Goodwin 1995; Mozley et al. 1995).

Predevelopment water levels (based on measurements made prior to 1961 in the vicinity of Albuquerque; Bexfield and Anderholm 2000) indicate that groundwater movement through the central part of the basin historically has been primarily oriented north to south (Fig. 2). Near the basin margins, groundwater flow historically has been primarily oriented toward the central part of the basin. There is a natural trough in the water-level surface (Bjorklund and Maxwell 1961; Titus 1961, 1963; Bexfield and Anderholm 2000) west of the Rio Grande, from just south of the Jemez River south to the area of Los Lunas (Figs. 1 and 2).

Data Collection

The data used in this investigation include new data specifically collected for this US Geol Surv MRGB study and historical (as early as 1941) groundwater and surface-water data from the US Geol Surv National Water Information System (NWIS) database and the city of Albuquerque. More than 300 sets of samples were collected at 288 groundwater sites (wells and springs) across the basin (Fig. 3) between June 1996 and August 1998. Well depths ranged from ~7–616 m, with a median of ~150 m. Screen lengths ranged from 1.5–387 m, with a median of 6 m. Water levels ranged from 1 to 336 m below land surface (b.l.s.), with a median water level of 55 m b.l.s. in a total of 263 measurements. The deepest unsaturated zones are in the northwestern part of the basin (median water level of 148 m b.l.s.), the west-central part of the basin (median water level of 100 m b.l.s.), and along the eastern basin margin (median water level of 110 m b.l.s.). In the Albuquerque vicinity, the groundwater data can represent conditions in about the upper 180–530 m of the saturated zone, but in areas outside of the Albuquerque vicinity, where there are fewer deep wells, the chemical and isotopic data generally are representative of conditions in the upper 60 m of the aquifer system. In any given location, the data are most representative of conditions in the part of the aquifer system used as the primary groundwater resource. All chemical and isotopic data are tabulated in Plummer et al. (2004), where details on methods of collection and analysis are given.

Chemical and Isotopic Composition of Groundwater in the Middle Rio Grande Basin

Chemical and isotopic data for groundwater of the MRGB were examined for relations and spatial patterns that could be useful in determining recharge sources, directions of groundwater flow, and geochemical processes. Data from available piezometer nests (mostly from the vicinity of Albuquerque) indicate that chemical patterns that can be mapped throughout the MRGB likely persist to depths of at least 200 m below the water table. However, some samples may be influenced by localized upward leakage of saline water along faults.

Inorganic Chemistry

Contours of specific conductance in groundwater of the MRGB (Fig. 4) indicate that the largest values (greater than 2,000 μS cm^{-1}) typically are near the western margin of the basin, where mineralized groundwater is thought to enter the basin from Paleozoic and Mesozoic rocks to the west. Values greater than about 1,000 μS cm^{-1} also are observed near the Hagan Embayment in the northeastern part of the basin, near the Tijeras Fault Zone along the eastern margin (Fig. 1), and at the southern end of the basin. The smallest values of specific conductance (less than 400 μS cm^{-1}) are along parts of the northern and eastern mountain fronts, and in an area extending across Rio Rancho and Albuquerque in the north-central part of the basin.

Most groundwater within the MRGB is slightly alkaline. Dissolved-oxygen concentrations greater than 2.0 mg L^{-1} are common in all parts of the basin except along the Rio Grande and along part of the western

 DOI 10.1007/s10040-004-0324-6

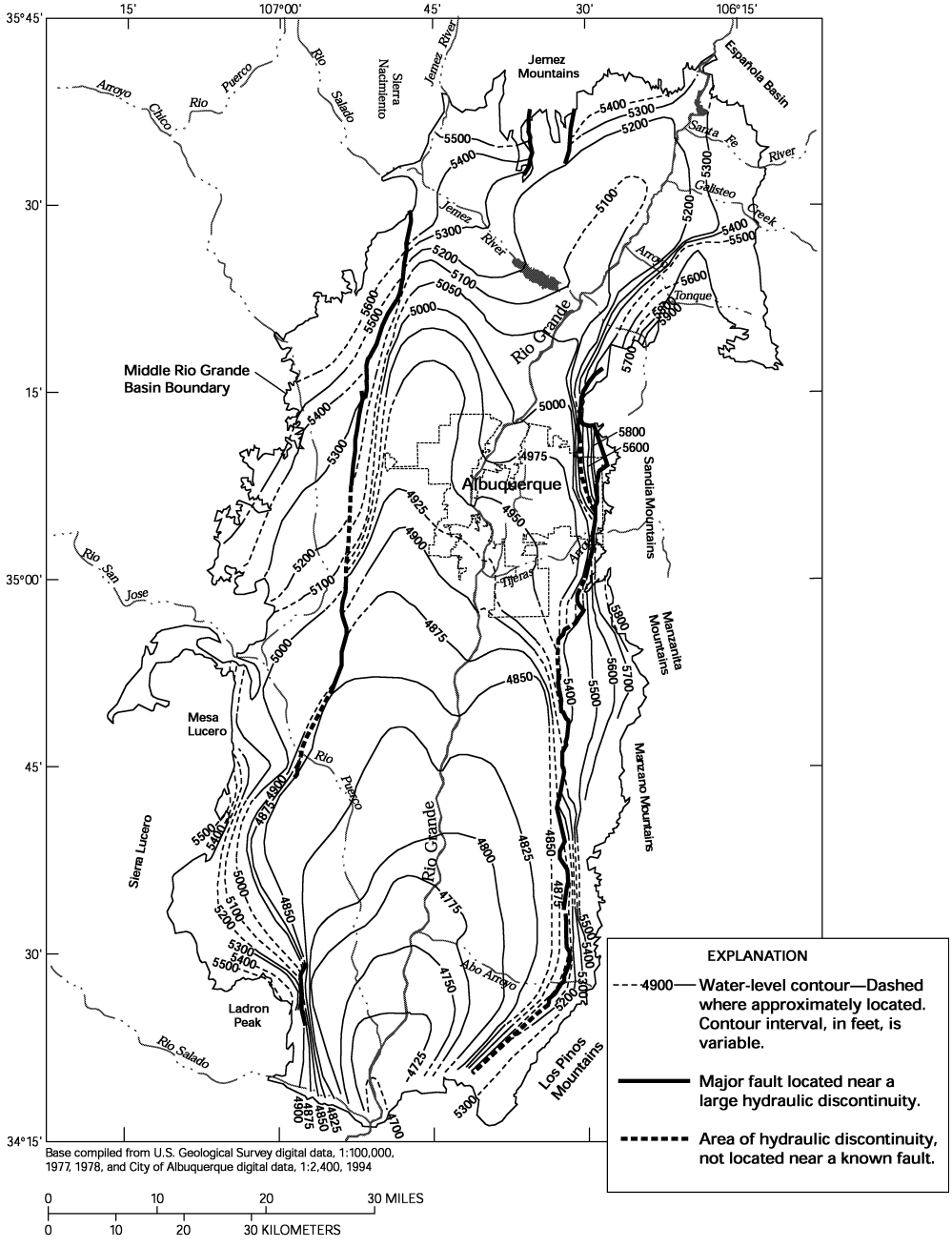

Fig. 2 Predevelopment water levels in the Middle Rio Grande Basin. Contours in feet (1 foot=0.3048 m) based on original source (Bexfield and Anderholm 2000)

margin, where concentrations typically are less than 0.5 mg L^{-1}. Water temperatures at the depths sampled in the MRGB generally range between 15–30 °C, with temperatures less than 20 °C along basin margins, along the Rio Grande, the Rio Puerco, Abo Arroyo, and across the northernmost section of the basin.

The most common water type among the groundwater samples analyzed is Ca-HCO_3, followed by Na-HCO_3 and mixed-cation-HCO_3. Different water types tend to group in distinct areas of the basin. With respect to cations, the Na-type generally dominates west of the Rio Grande (except near the northern end of the basin), whereas the Ca-type generally dominates east of the Rio Grande. Mixed-cation samples are relatively common near the Rio Puerco, in the southeastern part of the basin, and in some parts of Albuquerque. With respect to anions, the HCO_3-type dominates across much of the eastern and northern parts of the basin. The SO_4-type dominates in areas near Abo Arroyo and the Hagan Embayment, and across much of the western part of the basin; the mixed-anion type also is relatively common west of the Rio Grande. The Cl-type waters primarily are in the southwestern part of the basin. The major and minor element composition of groundwater was mapped throughout the basin (Plummer et al. 2004).

Most values of total alkalinity (as HCO_3) in waters from the center of the basin are less than 200 mg L^{-1}, and are commonly less than 150 mg L^{-1}. Larger values of

 DOI 10.1007/s10040-004-0324-6

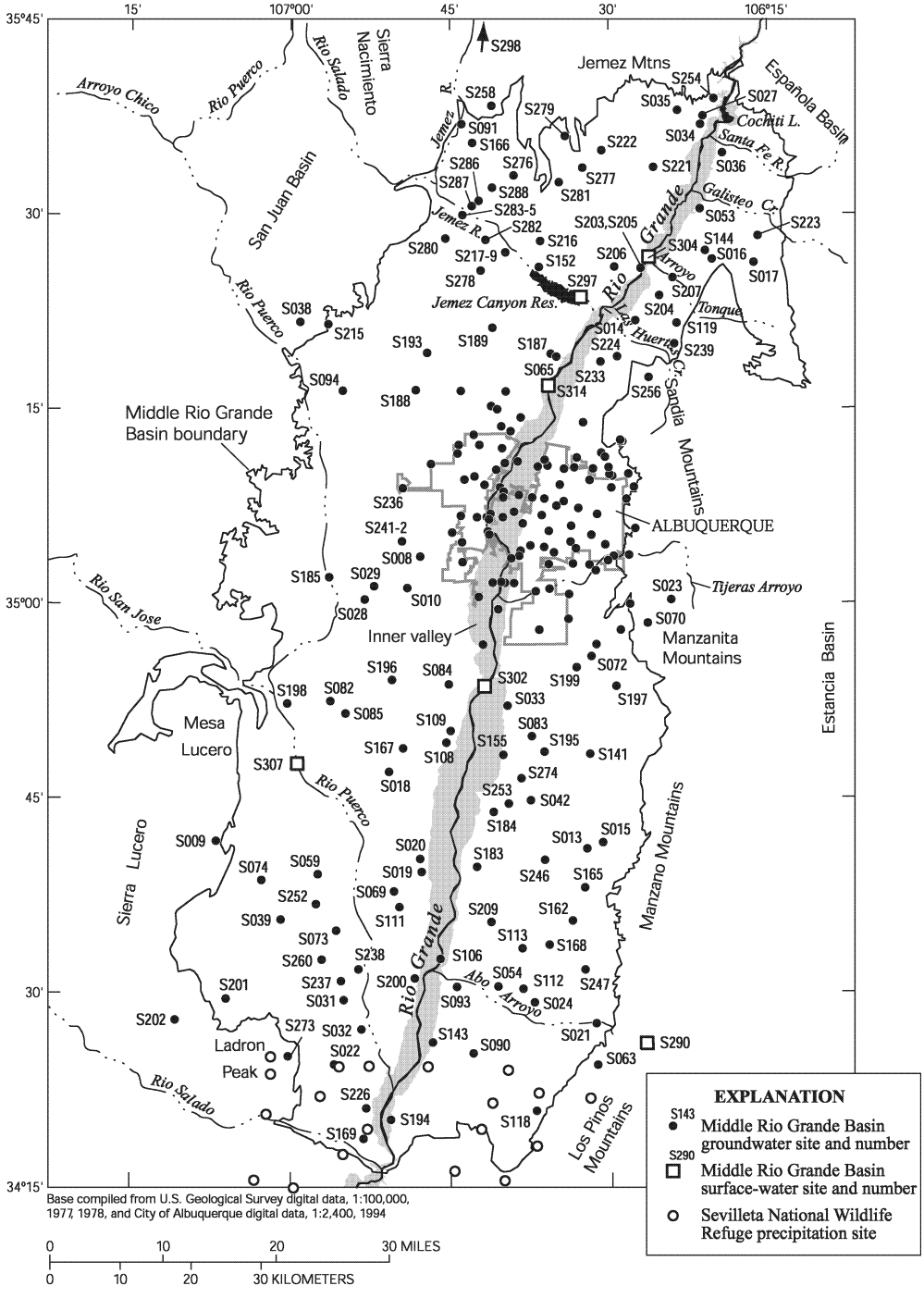

Fig. 3 Locations of groundwater and surface-water samples collected for the Middle Rio Grande Basin study area, and locations of precipitation samples collected in Sevilleta National Wildlife Refuge

alkalinity are along much of the eastern mountain front and near the western margin of the basin. Even in areas of smaller alkalinity values, calculations indicate that most groundwater samples are at or near saturation with respect to calcite. Approximately 250 measurements of $\delta^{13}C$ of the DIC in groundwater from the MRGB average –7.9±2.0 per mil. Over large sections of the basin, from approximately the Jemez River to the southern extent of the basin, $\delta^{13}C$ values are nearly constant along the generally north-to-south direction of regional groundwater flow. This indicates that geochemical reactions that could affect the dissolved inorganic carbon are not extensive.

Hydrogen-2 (δ^2H) and Oxygen-18 ($\delta^{18}O$) Isotopes in Groundwater

Albuquerque vicinity

Approximately 380 stable isotope measurements of groundwater in the vicinity of Albuquerque were obtained as a part of this study. Most groundwater beneath the

 DOI 10.1007/s10040-004-0324-6

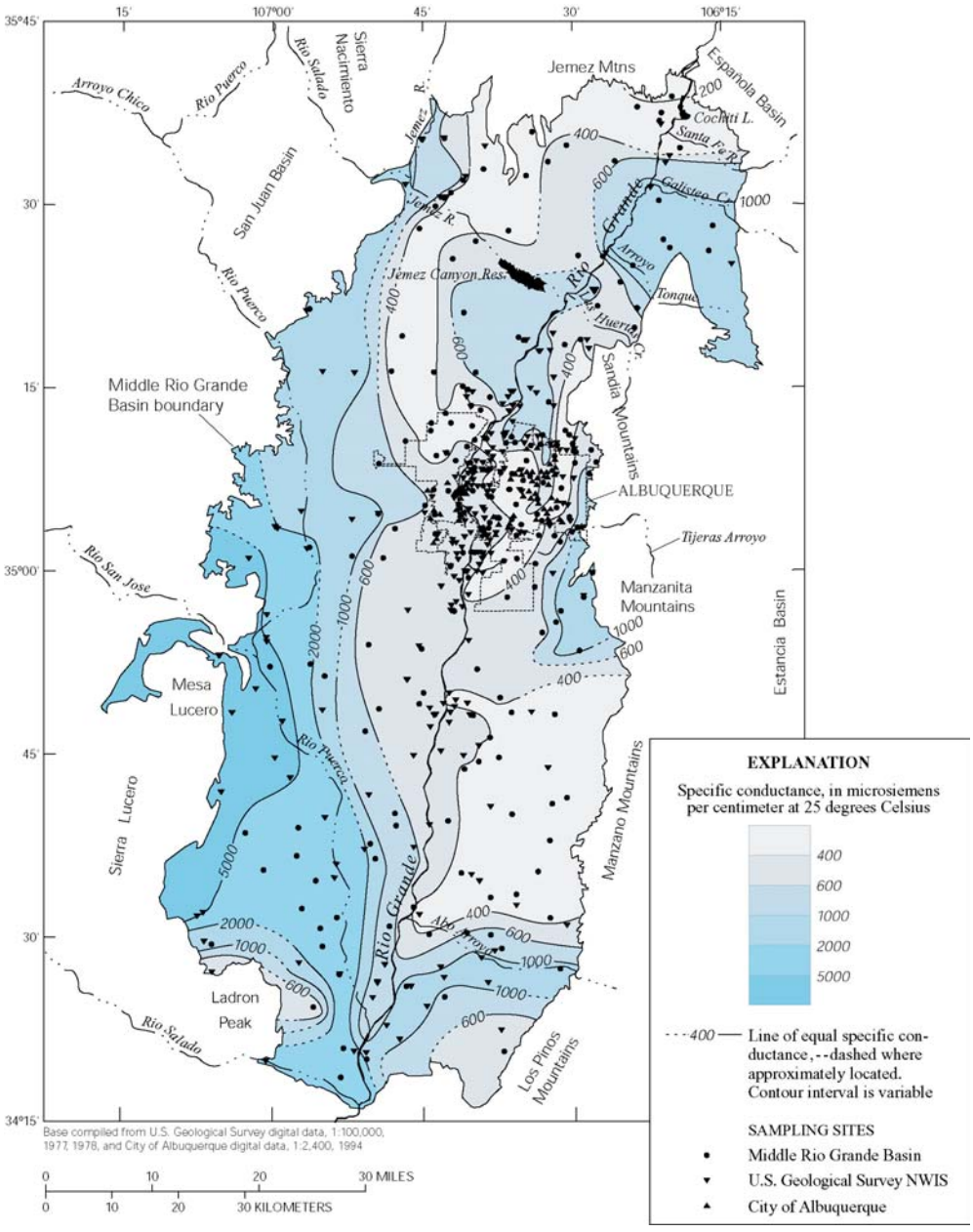

Fig. 4 Specific conductance of groundwater of the Middle Rio Grande Basin

eastern-most one-third of Albuquerque and north of Tijeras Arroyo has δ^2H values of –80 to –85 per mil (Fig. 5). This water is similar in isotopic composition to mountain-front recharge along the western side of the Sandia Mountains at Albuquerque (Yapp 1985; Plummer et al. 2004).

South of Tijeras Arroyo, in the region beneath most of Kirtland Air Force Base, the stable isotopic composition of groundwater is enriched in ^{2}H typically by 10 per mil or more relative to mountain-front recharge at Albuquerque. It is similar in isotopic composition to many of the surface-water samples from Tijeras Arroyo and water associated with the Tijeras Fault Zone southeast of Albuquerque (Figs. 1 and 5).

To the west of the Tijeras Arroyo vicinity, and beneath approximately the western two-thirds of the city of Albuquerque, the stable isotopic composition of groundwater becomes significantly depleted in ^{2}H. The transition to isotopically depleted water occurs over a narrow zone, which has a width less than approximately 2 km and strikes approximately north–south (Fig. 5). West of the transition zone, the δ^2H values of water typically are more negative than –90 per mil, in the range of –90 to –100 per mil. Some waters, in an area south and southwest of Albuquerque, have δ^2H values as negative as –110 per mil at the mid-depths of the wells at sites S004 and S005 (Fig. 5). Waters in the range of –90 to –100 per mil are similar in isotopic composition to that of the Rio Grande, as pointed out by Yapp (1985).

In sharp contrast to the relatively depleted waters observed throughout most of the vicinity of Albuquerque, some of the most enriched groundwater samples of the entire MRGB are at sites S103-S105, west of Corrales and northwest of Albuquerque, where δ^2H values of –56.6,

 DOI 10.1007/s10040-004-0324-6

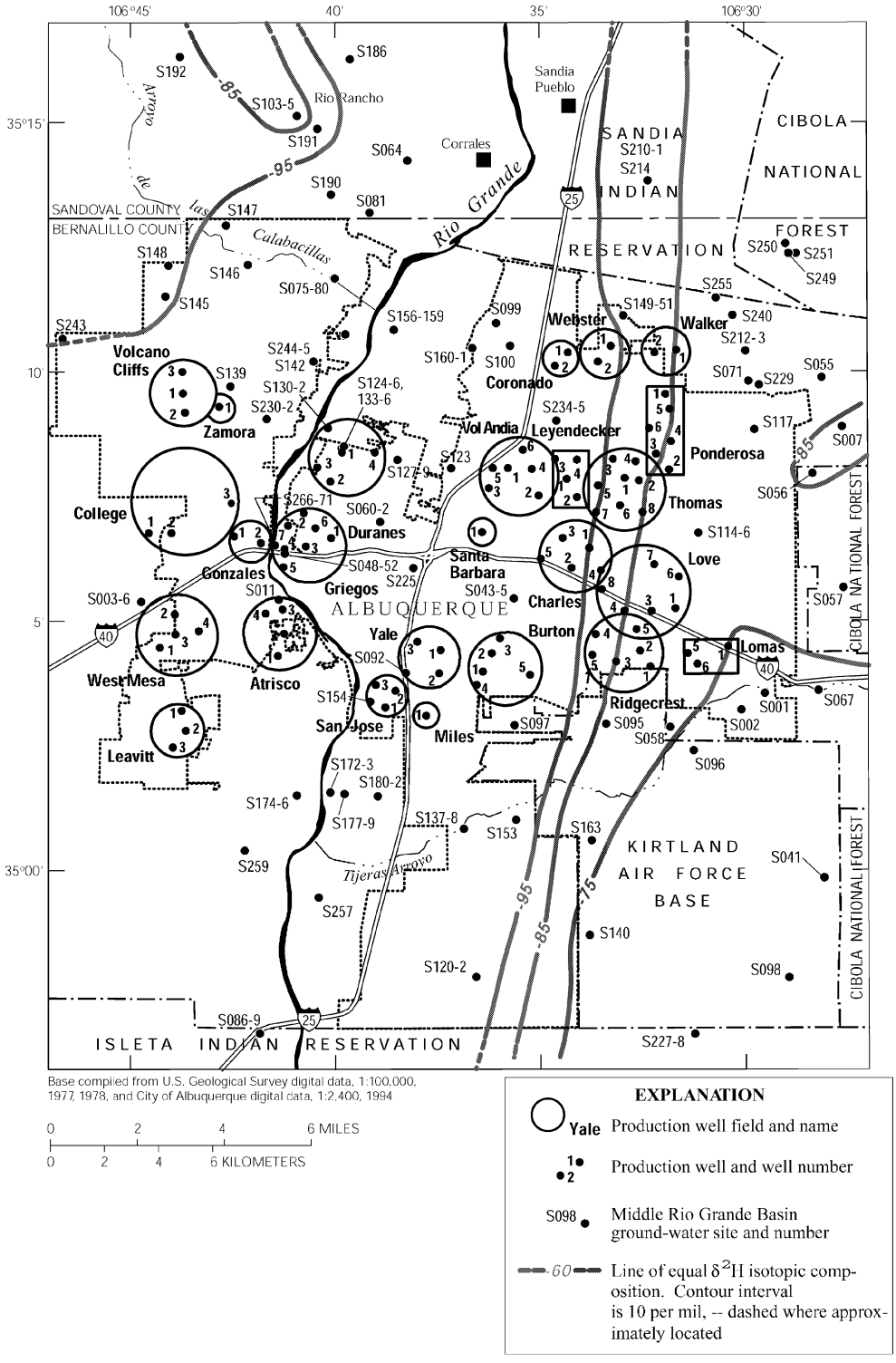

Fig. 5 Variations in δ^2H isotopic composition, in per mil, of groundwater in the vicinity of Albuquerque. *Circles and boxes* identify production well fields. The *closely spaced contours* on the east side of Albuquerque mark the boundary between the eastern mountain front zone to the east and the central zone (of Rio Grande origin) to the west

–56.5, and –67.3 per mil were observed at the shallow, medium, and deep completions, respectively (Fig. 5). The isotopically enriched ^{2}H and ^{18}O values in the samples do not appear evaporated, are observed over more than 300 m of aquifer thickness, and, as seen in a later section of this report, probably were recharged at relatively low altitudes in the northern part of the basin. The radiocarbon ages of the DIC in water from the shallow, medium, and deep completions at sites S103-S105 (Fig. 5) are 9.8, 15.0, and 15.9 ka, respectively.

Basin-wide

Approximately 100 analyses were obtained of the stable isotopic composition of groundwater basin-wide outside

 DOI 10.1007/s10040-004-0324-6

the Albuquerque area, predominantly from the upper 60 m of the aquifer system. Results from the few monitoring wells outside the Albuquerque area, such as the wells at sites S217, S288, S283, and S253 (Fig. 3), indicate that in parts of the basin, the patterns established in the upper 60 m of the aquifer system are representative of water to depths of at least 200 m below the water table, as was observed in many of the monitoring wells in the Albuquerque area. The lack of variation in stable isotopic composition with respect to depth suggests that the flow directions determined from water-quality data in the relatively shallow wells (most wells sampled) may extend some 450 m or more below the water table throughout much of the MRGB. There are a few exceptions to this observation of nearly constant stable isotopic composition with depth, such as along the northern part of the basin. In this area, isotopically enriched water recharged at low-altitude along the northern margin of the basin forms the uppermost part of the aquifer system (<50 m) and overlies at least 200 m of isotopically depleted paleo-water that can be traced throughout the west-central part of the basin, as discussed below.

The average δ^2H composition of water from the wells sampled outside the vicinity of Albuquerque is –82.1 per mil, compared with waters sampled from the Albuquerque vicinity, which average –92.4 per mil in δ^2H. Water in the vicinity of Albuquerque is more depleted in comparison to waters basin-wide because water from the relatively depleted Rio Grande contributes to a larger number of wells in the Albuquerque area than basin-wide. The range of δ^2H values of all the water sampled outside the Albuquerque area is 65 per mil (–118.3 to –52.9 per mil), compared with 38 per mil (–111.3 to –73.7 per mil) in the Albuquerque area, and was fitted to the line $\delta^2H=7.6\delta^{18}O+2.5$ (Fig. 6).

Like many of the major water-quality parameters, the stable isotopic composition of groundwater can be contoured throughout most of the MRGB (Fig. 7). Important features of the stable isotope contour map are the following. (1) Contours in stable isotope composition tend to align north to south in the central part of the basin, parallel to the direction of the general north-to-south flow of groundwater. (2) A zone of isotopically depleted water extends over the west-central part of the northern two-thirds of the basin, and is beneath relatively enriched waters in the northern-most part of the basin. (3) An area of isotopically enriched water extends along the western and southwestern parts of the basin. (4) A zone of water with δ^2H values in the –90s per mil range extends north–south along both sides of the Rio Grande throughout most of the basin. (5) Water with δ^2H values in the –70s and –80s per mil range is along the eastern and northern margins of the basin (Fig. 7).

Based on stable isotope data, it appears that the "deuterium-depleted deep water", first recognized by Yapp (1985) in southwestern parts of Albuquerque in waters with δ^2H values of approximately –102 per mil, is part of a regional pattern in depleted stable isotope composition of water that extends through the west-central part of the basin from the northernmost boundary (at depth) south to an area in the vicinity of Belen. The "deuterium-depleted deep water" was observed in water from two wells at Rio Rancho (sites S193 and S188; Fig. 3), approximately 32 km northwest of Albuquerque, and is in deep monitoring wells in the northern part of the basin (sites S288, S283-S284, and S217-S219, Fig. 3) to depths of more than 300 m below the water table. The "deuterium-depleted deep water" is beneath a relatively thin zone of somewhat enriched water (δ^2H values in the –80s per mil range) along the northern margin of the basin at sites S288, S283-S284, and S217-S219. Along the Rio Grande in the central part of the basin, the "deuterium-depleted deep water" is beneath water of Rio Grande composition (δ^2H values in the –90s per mil range) such as at sites S004-S005 and sites S120-S121. The "deuterium-depleted deep water" appears to merge with multiple sources of groundwater in the Rio Grande south of Abo Arroyo, in the southern part of the basin (Fig. 7).

West of the central area of "deuterium-depleted deep water", the stable isotopic composition of groundwater is greatly enriched by comparison. The enriched western waters parallel the Rio Puerco in the western and southwestern parts of the basin. The isotopic composition of this groundwater is similar to values measured for water from the Rio Puerco (Plummer et al. 2004), and it is likely that infiltration from the Rio Puerco contributes part of the water observed in the western and southwestern parts of the basin.

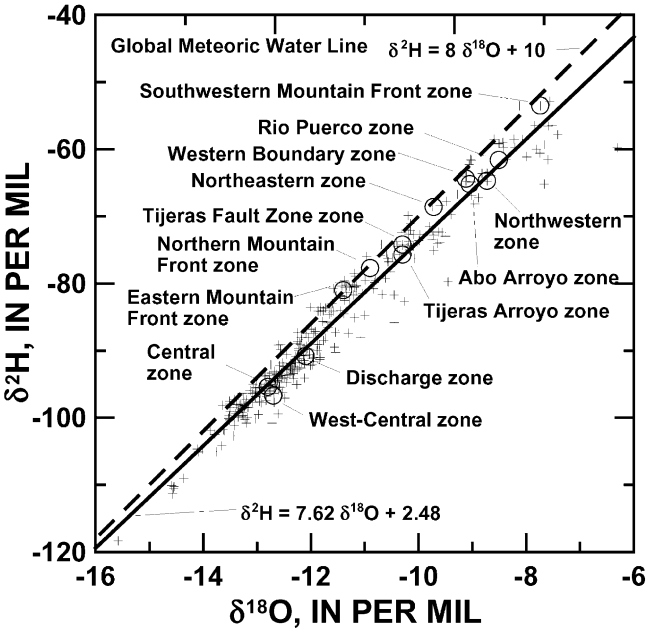

Fig. 6 Values of δ^2H and δ^{18}O isotopic composition for all groundwater samples from the Middle Rio Grande Basin, New Mexico, in relation to the global meteoric water line. The *solid line* shows a least squares fit to the groundwater data. The *circles* locate median stable isotopic composition of water from each hydrochemical zone (Tables 1 and 2)

 DOI 10.1007/s10040-004-0324-6

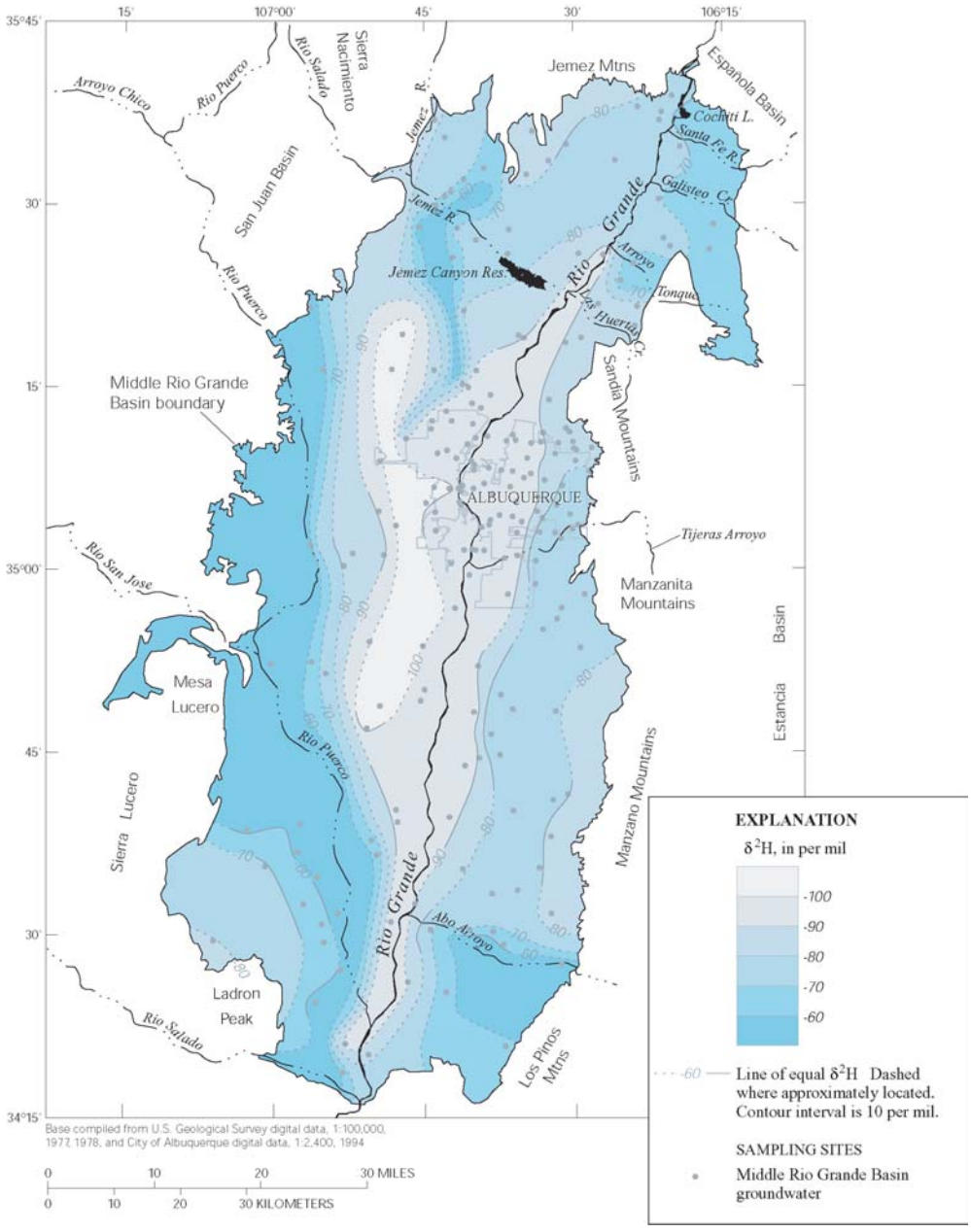

Fig. 7 Variations of δ^2H isotopic composition of groundwater in per mil from the Middle Rio Grande Basin

Water along the northern, eastern, and southwestern margins of the basin tends to have values of δ^2H in the range of –80s per mil that are indicative of mountain-front recharge. The most enriched waters in the southwestern part of the basin are in the vicinity of the Rio Puerco and arroyos along the southwestern basin margin.

The sharp boundary between mountain-front recharge (δ^2H values in the –80s per mil) and Rio Grande water (δ^2H values in the –90s per mil) observed at Albuquerque (Figs. 5 and 7) appears to extend north through Sandia Pueblo to San Felipe Pueblo, where the depleted Rio Grande stable isotope signal pinches out at the Rio Grande. The stable isotope pattern is consistent with the suggestion of Yapp (1985) that, north of San Felipe, there may be net discharge of groundwater to the Rio Grande, but further south from San Felipe, there is net loss of Rio Grande water to the aquifer system. Based on stable isotope data, the zone of influence of infiltration from the Rio Grande is more than ~16 km in width just north of Albuquerque, remains about 16 km wide through most of Albuquerque, and then narrows south of Albuquerque parallel to the Rio Grande (Fig. 7). Waters with stable isotopic composition similar to the Rio Grande appear to mix with other western, northern, and eastern sources of water in the southernmost part of the basin.

Although stable isotopes can be extremely useful in recognizing sources of water to the MRGB, it could be quite misleading to base such interpretation solely upon stable isotope data, without considering all available chemical and isotopic data.

 DOI 10.1007/s10040-004-0324-6

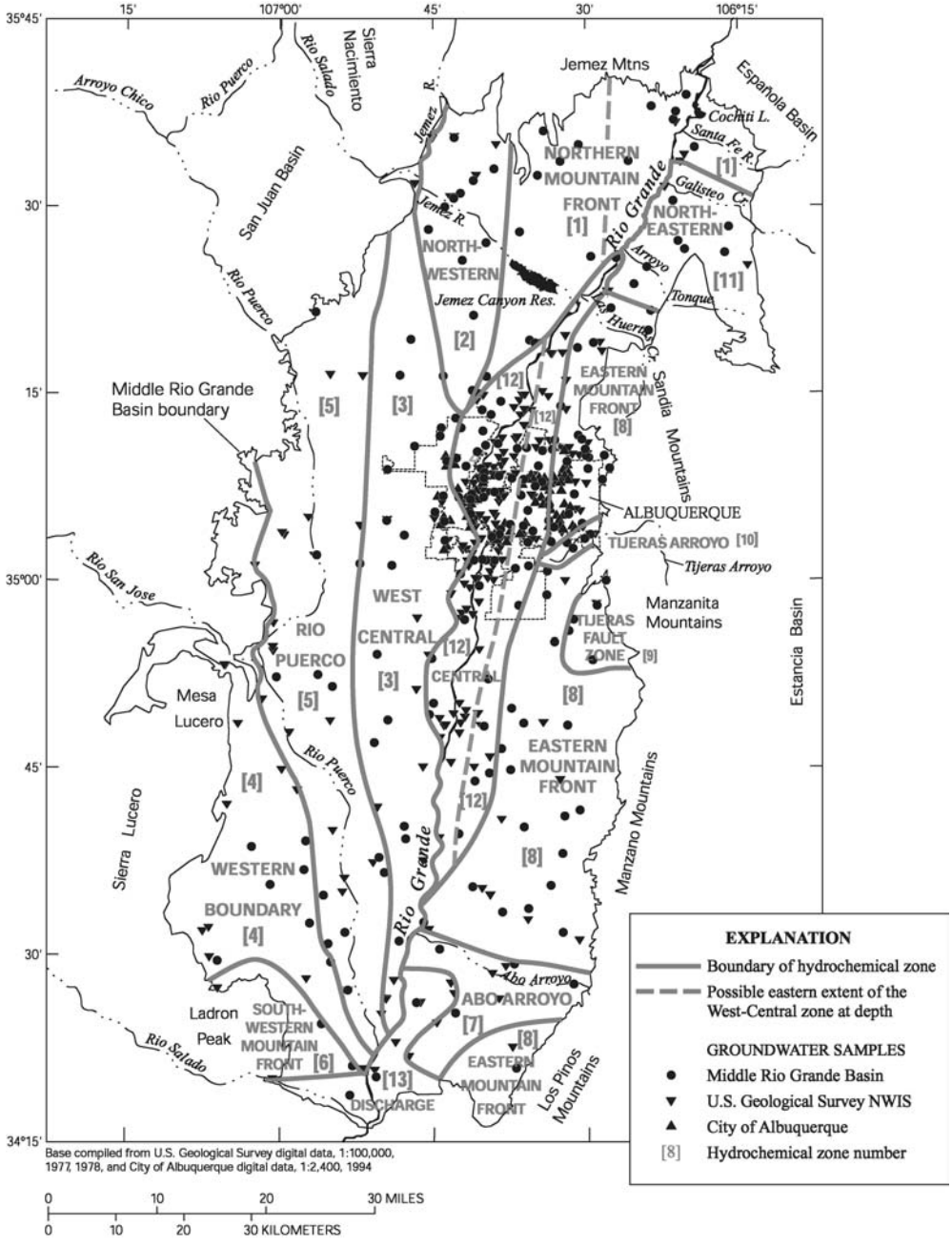

Fig. 8 Hydrochemical zones defined for the Middle Rio Grande Basin. The *dashed lines* represent the possible extent of the West-Central zone at depth beneath other zones

Tracing Sources of Water in the Middle Rio Grande Basin: Definition of Hydrochemical Zones and Water Sources

Distinct spatial patterns in the chemical and isotopic composition of groundwater in the MRGB have been recognized and mapped in various parts of the basin (Yapp 1985; Anderholm 1988; Logan 1990; Plummer et al. 2001, 2004). The patterns in chemical and isotopic composition of MRGB groundwater were used to define 13 hydrochemical zones (Fig. 8), 12 of which represent separate sources of recharge to the basin (zones 1–12), and one zone of discharge (zone 13) (Plummer et al. 2001, 2004). The hydrochemical zones were assigned geographical names (and hydrochemical zone numbers) based either on position within the basin (Northeastern: zone 11; Northwestern: zone 2; Western Boundary: zone 4; West-Central: zone 3; Central: zone 12; Northern Mountain Front: zone 1; Eastern Mountain Front: zone 8; Southwestern Mountain Front: zone 6; and Discharge zone: zone 13) or on a major hydrologic or geologic feature of the area (Rio Puerco: zone 5; Abo Arroyo: zone 7; Tijeras Arroyo: zone 10; and Tijeras Fault Zone zone 9). The hydrochemical zones defined in this study (Fig. 8) provide insight into likely recharge sources, flow paths, and aquifer properties.

Each groundwater sample in the data set for the basin was assigned to a particular hydrochemical zone based on

 DOI 10.1007/s10040-004-0324-6

location and chemical and isotopic composition (see Appendix A of Plummer et al. 2004). Although Fig. 8 provides a reasonable two-dimensional representation of zone boundaries, the data show that zone boundaries are not strictly vertical within the aquifer system. For example, as defined, the West-Central zone actually extends at depth beneath essentially the entire Northwestern zone and may extend beneath parts of the Northern Mountain Front and Central zones. In some instances, samples from different depths within the same well nest were assigned to different zones. Therefore, in Fig. 8, a sample assigned to a particular zone can appear to be located in an adjacent zone because of depth considerations. Finally, the boundaries shown between zones are not meant to indicate extremely sharp shifts in water chemistry, but rather areas of greatest transition between two different water types.

Median values of selected parameters are summarized in Table 1 for each hydrochemical zone. The Mann–Whitney statistical test (otherwise known as the Wilcoxon rank-sum test) was applied to selected chemical and isotopic data from adjacent zones to determine whether the samples actually could have come from separate populations. The test calculates whether the median values from the two groups being compared are statistically different, or whether they could represent the medians of two groups drawn from the same population. The test is non-parametric and so does not require the statistical distributions of the groups being compared to have the same shape or variability (Helsel and Hirsch 1995). The Mann–Whitney test was used to compare only those hydrochemical zones that contained at least ten samples for most constituents, which included every zone except the Southwestern Mountain Front and Discharge zones. Selected parameters for which the test showed statistically different medians between zones at the 95% confidence level are listed in Table 2.

Waters from the Northern Mountain Front, Northwestern, Eastern Mountain Front, and Southwestern Mountain Front zones have compositions that are characteristic of mountain-front recharge. Waters in the West-Central zone are depleted in ^{2}H, have generally low ^{14}C activity, and appear to have been recharged along relatively high-altitude flanks of the Jemez Mountains during the last glacial period (Plummer et al. 2004). Several zones appear to contain significant fractions of groundwater inflow from adjacent basins. The Western Boundary zone contains groundwater inflow from the Mesozoic and Paleozoic rocks west of the basin that have mixed with local arroyo recharge. The Northeastern zone contains inflow from the Hagan Embayment that has mixed with local arroyo recharge and mountain-front recharge sources.

Several zones are dominated by infiltration of surface-water sources. Water in the Central zone is predominantly of Rio Grande origin, but zones dominated by recharge from Abo Arroyo, the Rio Puerco, and Tijeras Arroyo are named for their primary source of recharge. Potential sources of recharge to the Tijeras Fault Zone zone include mountain-front recharge along the Manzanita Mountains and inflow of deep groundwater across the eastern basin margin. Possible sources of water to the Discharge zone, in the southern tip of the basin (Fig. 8), include several of the upgradient hydrochemical zones, including the Southwestern, Western Boundary, Rio Puerco, Central, Eastern Mountain Front, and Abo Arroyo zones. These sources of water span a relatively large range in stable isotopic composition (Fig. 6); however, the relatively depleted isotopic composition of water from the Discharge zone indicates that groundwater discharge from the basin is predominantly of depleted sources, such as water from the Central and West-Central zones. Groundwater of the Discharge zone probably discharges to the Rio Grande or to the Socorro Basin to the south.

Radiocarbon Data and Interpretation of Radiocarbon Age

Spatial Patterns in ^{14}C Activity

The measured ^{14}C activities of DIC of groundwater from 211 sites (excluding duplicate samples) in the MRGB range from 0.62–123.1 pmC. A smooth continuum of ^{14}C activity is apparent throughout the basin (Fig. 9). Most of the contours in ^{14}C activity align in a north–south direction that roughly parallels the water source. ^{14}C activities are highest along the eastern mountain front, along the northern margin of the basin, along the southwestern margin of the basin associated with recharge from Ladron Peak (Fig. 1), and along the inner valley of the Rio Grande, corresponding to areas of recharge during the past 5–10 ka. Relatively high ^{14}C activities also are near areas where Abo Arroyo, the Rio Puerco, and the Jemez River enter the basin (Fig. 9). Waters with low values of ^{14}C activity of DIC are along the western and southwestern basin margins. A zone of low ^{14}C activity extends through nearly the entire length of the west-central part of the basin. The ^{14}C activities generally indicate that waters in the MRGB have ages on a time scale of tens of thousands of years.

Initial ^{14}C Activity of DIC, A_o

Calculation of radiocarbon age from the measured ^{14}C activity requires estimation of the ^{14}C activity in the recharge areas, A_o, and evaluation of the effects of geochemical reactions along flow paths in the aquifer (Wigley et al. 1978; Plummer et al. 1994; Kalin 2000). In this study, actual measured values of ^{14}C activity in DIC from recharge areas permitted definition of A_o. Water samples from recharge areas that contained ^{3}H or CFCs had ^{14}C activities in the range of 95-120 pmC, and were consistent with the assumption of open-system evolution. The ^{14}C activity of DIC in two samples of water from the Rio Grande at San Felipe and Alameda, north of Albuquerque, from 29 June 1996, were 96.05±0.69 and 97.13±0.98 pmC, respectively. If the pre-1950s recharge water formed under open-system conditions, A_o would be

 DOI 10.1007/s10040-004-0324-6

Table 1 Median values of selected water-quality parameters by hydrochemical zone. – No data; *µS/cm* microsiemens per centimeter at 25°C; *mg/L* milligrams per liter; *µg/L* micrograms per liter; *pmC* percent modern carbon

Hydrochemical Zone	Specific conductance (µS/cm)	pH, field (standard units)	Water temperature (deg. C)	Dissolved oxygen (mg/L)	Calcium (mg/L Ca)	Magnesium (mg/L Mg)	Sodium (mg/L Na)	Potassium (mg/L K)	Alkalinity (mg/L HCO_3)	Sulfate (mg/L SO_4)	Chloride (mg/L Cl)	Fluoride (mg/L F)	Bromide (mg/L Br)	Silica (mg/L SiO_2)	Nitrate (mg/L N)	Aluminum (µg/L Al)	Arsenic (µg/L As)
Northern Mountain Front	340	7.49	18.9	5.12	38.5	6.1	20.0	4.9	137.	19.5	5.6	0.35	0.08	53.3	0.56	---	3.2
Northwestern	400	7.84	20.6	6.68	33.9	4.2	49.9	5.7	160.	44.8	8.5	0.61	0.07	30.1	2.44	---	9.8
West Central	535	8.22	23.8	3.00	12.0	2.5	103.	4.2	174.	92.0	13.4	0.99	0.11	34.5	1.24	6.76	23.2
Western Boundary	4,572	7.70	22.0	4.09	135.	56.4	589.	15.2	300.	793.	820.	1.64	0.38	22.5	0.86	5.00	1.8
Rio Puerco	2,731	7.50	20.0	3.73	135.	42.7	290.	10.4	190.	1,080.	185.8	0.63	0.64	21.8	0.88	5.00	1.0
Southwestern Mountain Front	462	8.11	19.1	4.43	52.6	13.5	27.8	2.5	202.	53.0	15.0	1.02	0.21	17.6	1.12	3.31	0.2
Abo Arroyo	1,055	7.45	20.7	6.23	92.5	34.4	49.2	3.1	148.	346.	25.9	0.90	0.17	24.0	1.40	4.14	5.2
Eastern Mountain Front	382	7.67	22.0	5.16	45.0	5.1	29.2	2.2	157.	31.0	10.5	0.60	0.17	28.4	0.31	5.56	2.0
Tijeras Fault Zone	1,406	7.42	18.5	4.66	171.	36.0	95.0	6.1	599.	100.	139.	1.27	0.69	18.9	1.09	5.22	2.2
Tijeras Arroyo	677	7.39	16.1	6.97	89.4	24.5	29.3	3.8	240.	115.	56.6	0.60	0.35	19.5	3.79	4.09	1.0
Northeastern	1,221	7.50	19.4	6.44	141.	29.5	81.8	4.8	208.	390.	22.7	0.51	0.19	38.5	0.64	4.34	2.7
Central	436	7.74	18.1	0.12	42.9	8.0	31.0	6.4	158.	66.0	16.6	0.44	0.09	47.0	0.08	6.00	5.4
Discharge	1,771	7.70	20.6	0.08	93.0	31.0	190.	10.5	157.	290.	280.	1.40	0.47	39.0	0.42	4.50	9.9

Hydrochemical Zone	Barium (mg/L Ba)	Boron (mg/L B)	Chromium (µg/L Cr)	Copper (µg/L Cu)	Iron (mg/L Fe)	Lead (µg/L Pb)	Lithium (mg/L Li)	Manganese (mg/L Mn)	Molybdenum (µg/L Mo)	Strontium (mg/L Sr)	Uranium (µg/L U)	Vanadium (µg/L V)	Zinc (µg/L Zn)	δD (per mil)	$\delta^{18}O$ (per mil)	$\delta^{13}C$ (per mil)	^{14}C (pmC)
Northern Mountain Front	0.062	0.043	1.2	0.8	0.060	0.20	0.058	0.005	1.7	0.31	1.0	6.4	258.	-77.7	-10.9	-8.50	33.4
Northwestern	0.056	0.118	2.0	0.4	0.030	0.10	0.068	0.002	3.4	0.57	2.7	15.6	9.0	-64.7	- 8.73	-6.93	29.6
West Central	0.032	0.239	5.7	0.5	0.028	0.11	0.045	0.002	8.2	0.20	3.7	27.9	5.0	-96.7	-12.7	-7.18	8.80
Western Boundary	0.014	0.900	10.6	3.0	0.213	0.12	0.251	0.041	9.9	2.09	4.4	5.7	118.	-64.4	- 9.12	-4.70	6.19
Rio Puerco	0.014	0.291	3.0	3.4	0.130	0.10	0.253	0.015	7.0	3.92	6.0	3.4	117.	-61.6	- 8.51	-7.65	36.4
Southwestern Mountain Front	0.045	0.094	1.9	9.3	0.030	0.41	0.041	0.007	3.0	0.86	0.9	1.0	252.	-53.5	- 7.74	-5.76	40.0
Abo Arroyo	0.017	0.130	4.4	2.0	0.105	0.10	0.031	0.004	3.4	1.48	5.4	9.5	8.1	-65.2	- 9.05	-6.72	24.1
Eastern Mountain Front	0.084	0.050	1.0	1.7	0.031	0.27	0.020	0.003	2.0	0.32	3.6	7.5	6.7	-81.0	-11.4	-8.70	47.2
Tijeras Fault Zone	0.046	0.347	1.7	4.3	0.111	0.34	0.227	0.023	3.7	1.11	7.3	6.3	61.5	-74.2	-10.3	-0.98	9.70
Tijeras Arroyo	0.057	0.060	1.1	1.0	0.050	0.10	0.017	0.005	1.9	0.47	3.7	3.0	4.5	-75.7	-10.3	-6.80	72.8
Northeastern	0.018	0.215	3.2	3.7	0.170	0.11	0.040	0.004	6.7	1.72	8.5	3.8	99.5	-68.6	- 9.72	-6.40	28.5
Central	0.083	0.085	1.0	0.8	0.041	0.10	0.040	0.015	5.0	0.40	3.6	9.3	5.0	-95.4	-12.8	-8.87	61.0
Discharge	0.030	0.630	10.2	1.7	0.080	0.15	0.326	0.010	10.3	3.02	3.9	7.1	16.2	-90.8	-12.1	-7.00	10.8

DOI 10.1007/s10040-004-0324-6

Hydrogeology Journal (2004) 12:359–388

Table 2 Parameters for which the Mann–Whitney test indicated statistically different medians between adjacent hydrochemical zones at the 95% confidence level. *X* indicates that medians for that parameter were statistically different for the zones listed

Hydrochemical zones compared	Specific conduct-ance	pH field	Water temper-ature	Dissol-ved oxygen	Calcium	Magne-sium	Sodium	Potas-sium	Alkalin-ity	Sulfate	Chlor-ide	Fluor-ide	Brom-ide	Silica	Nitrate	Alum-inum
Northern Mountain Front and Northwestern		X		X						X		X		X	X	
Northwestern and West Central	X	X	X	X	X	X	X			X		X	X		X	X
West Central and Rio Puerco	X	X	X		X	X	X	X		X	X		X	X		
Western Boundary and Rio Puerco	X						X	X	X		X	X				
Abo Arroyo and Eastern Mountain Front	X				X	X	X			X	X				X	
Eastern Mountain Front and Tijeras Fault Zone	X	X	X		X	X	X	X	X	X	X	X	X	X	X	
Eastern Mountain Front and Tijeras Arroyo	X	X	X		X	X		X	X	X	X			X	X	
Tijeras Fault Zone and Tijeras Arroyo	X			X		X	X		X		X	X			X	
Northeastern and Eastern Mountain Front	X		X		X	X	X	X	X	X	X			X		X
Northeastern and Northern Mountain Front	X				X	X	X		X	X	X	X	X			
Central and Eastern Mountain Front	X		X	X		X		X		X	X	X	X	X	X	
Central and Northern Mountain Front	X	X		X	X	X				X	X				X	X
Central and West Central	X	X	X	X	X	X	X	X		X	X	X		X	X	

Hydrochemical zones compared	Arsenic	Barium	Boron	Chrom-ium	Copper	Iron	Lead	Lith-ium	Manga-nese	Molyb-denum	Stront-ium	Uran-ium	Vanad-ium	Zinc	δD	^{14}C	$\delta^{13}C$
Northern Mountain Front and Northwestern			X			X					X		X		X		
Northwestern and West Central	X	X	X	X						X	X		X		X	X	
West Central and Rio Puerco	X	X			X	X		X	X	X	X		X	X	X	X	
Western Boundary and Rio Puerco			X													X	X
Abo Arroyo and Eastern Mountain Front		X	X	X			X				X				X		X
Eastern Mountain Front and Tijeras Fault Zone			X			X		X	X		X	X				X	X
Eastern Mountain Front and Tijeras Arroyo	X						X				X				X		X
Tijeras Fault Zone and Tijeras Arroyo	X		X					X	X	X	X					X	
Northeastern and Eastern Mountain Front		X	X	X		X				X	X			X	X		X
Northeastern and Northern Mountain Front			X		X					X	X	X			X		X
Central and Eastern Mountain Front	X		X		X	X	X	X	X	X	X			X	X		
Central and Northern Mountain Front			X						X	X		X		X	X		
Central and West Central	X	X	X	X					X	X	X		X			X	X

DOI 10.1007/s10040-004-0324-6

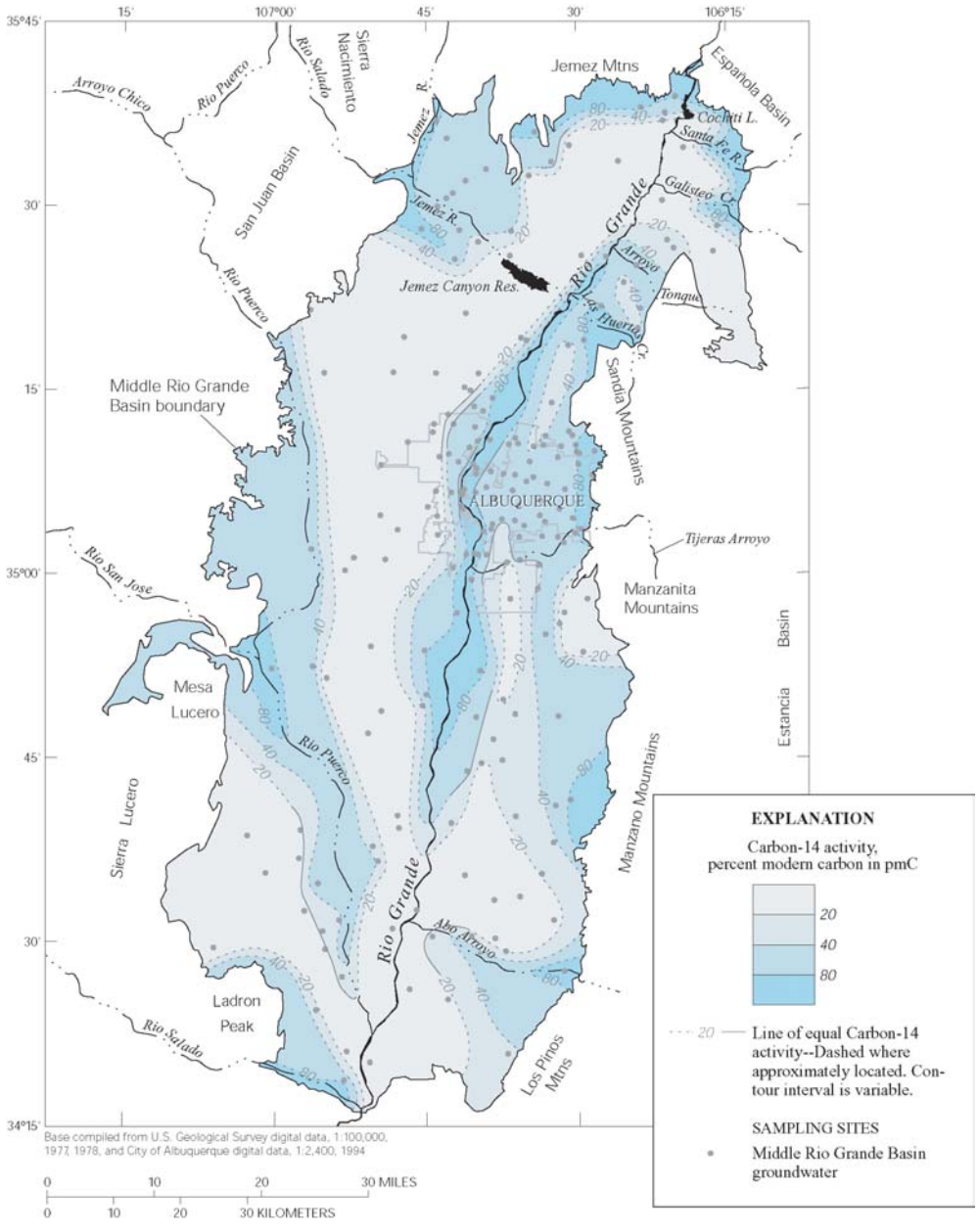

Fig. 9 Variations of ^{14}C activity in percent modern carbon, pmC, for dissolved inorganic carbon from groundwater samples from the uppermost approximately 60 m of the aquifer system, Middle Rio Grande Basin

expected to be near 102 pmC, assuming that the ^{14}C activity of the unsaturated-zone CO_2 was 100 pmC, and the equilibrium fractionation factor for ^{14}C between CO_2 gas and HCO_3^- is twice the ^{13}C equilibrium fractionation factor. The distribution of ^{14}C activities in mountain-front areas and in recent seepage from the Rio Grande suggests that A_o is likely in the range of 95–102 pmC (Plummer et al. 2004). Throughout this report, a value of A_o equal to 100 pmC is assumed. The unadjusted radiocarbon ages of this report would be decreased by 400 years if calculated using a value of A_o of 95 pmC instead of 100 pmC.

Geochemical Reactions

Possible reactions that can affect the ^{14}C activity of DIC in the MRGB include dissolution of carbonate minerals (primary and secondary calcite, caliche), calcite precipitation, carbon isotopic exchange with calcite, and oxidation of organic matter. Cation-exchange reactions, in which Ca^{2+} is taken up on clay surfaces in exchange for Na^+, will lower the calcite saturation state and permit additional dissolution of calcite, if calcite is present locally in the aquifer mineralogy. Anderholm (1985) showed that calcium smectite and mixed-layer illite–smectite clays, both of which have large ion-exchange capacities, are present in the Santa Fe Group aquifer system. The dissolution of calcite accompanying ion exchange dilutes the ^{14}C activity of DIC in the groundwater,

 DOI 10.1007/s10040-004-0324-6

and if not accounted for in age interpretation, the radiocarbon age is biased old.

Weathering of primary silicates, such as plagioclase feldspars, releases Ca^{2+} to groundwater and raises the pH, both of which can cause calcite to precipitate. Due to isotope fractionation, ^{14}C is slightly enriched in calcite precipitates relative to its isotopic abundance in the dissolved phase. Not correcting for this causes calculated radiocarbon ages to be biased old; however, the effect of silicate weathering and $CaCO_3$ precipitation on radiocarbon ages generally is negligible compared to dissolution of calcite.

NETPATH Models

The geochemical mass-balance code, NETPATH (Plummer et al. 1994), was used to construct mass-balance models for the origin of waters in the basin and to investigate the sensitivity of the unadjusted radiocarbon ages to effects of possible geochemical reactions. NETPATH uses equations of chemical mass balance, electron balance, and isotope mass balance to define possible net geochemical reactions between source waters and the observed groundwater compositions along a flow path. Because pairs of samples generally cannot be identified along a specific flow path in the MRGB, representative source-water compositions were selected for each hydrochemical zone (Table 3). The geochemical reactions were constrained among reasonable reactant and product minerals and gases for the aquifer system, and to be consistent with the observed mineralogy, chemical, and isotopic data. Each geochemical reaction model also was solved as an isotope-evolution problem (Wigley et al. 1978, 1979), accounting for various isotopic sources and isotope fractionation along the reaction path to predict the isotopic composition at the end point in the reaction, including adjustment of A_o for geochemical reactions.

Each groundwater sample in the MRGB was assumed to have evolved from a primary source-water composition that was subsequently altered to varying degrees by:

1. Evapotranspiration/dilution processes.
2. Mixing with surface water(s).
3. Mixing with saline upward leakage water(s).
4. Mixing with groundwater inflow from adjacent basins.
5. Water/rock reaction.

A primary source water was uniquely specified for each hydrochemical zone. For example, groundwater from the Eastern Mountain Front zone was assumed to have evolved geochemically from the representative Eastern Mountain Front source water (Table 3). The compositions of all source waters and other secondary source waters used in the geochemical models are listed in Table 3. In many cases, the chemical compositions of the source waters represent averages of sample compositions from the US Geol Surv NWIS surface-water database. In the cases of source waters "ASSP", "saline water 1" and "saline water 2" (Table 3), the compositions are those of individual samples collected as a part of this investigation.

Phases considered in the geochemical models as possible reactants and products included calcite, plagioclase feldspar (AN_{38}), carbon-dioxide gas, kaolinite, silica, gypsum, Ca/Na exchange, and, in areas undergoing redox reactions, organic carbon (designated CH_2O for carbon of oxidation state zero). No important reactant or product minerals containing magnesium were recognized in the MRGB, and none of the models were constrained by the magnesium data. The compositions of phases used in the models were selected to be representative of groups of phases present in the MRGB. The models also included the possibility of conservative concentration or dilution of source-water solute content — the evapotranspiration/dilution factor. A value of the evapotranspiration/dilution factor less than 1 indicates dilution of the source water(s), or paleo-source-water compositions that were more dilute than the average compositions used here (Table 3). Similarly, values of the evapotranspiration/dilution factor greater than 1 indicate concentration of the source water solutes such as in evapotranspiration, or paleo-source-water compositions that had greater solute content than the average compositions used in the geochemical calculations (Table 3).

The initial ^{14}C activity of source waters was assumed to be 100 pmC for DIC in mountain-front recharge (as discussed above), and was the measured value for surface waters and samples ASSP, saline water 1 and saline water 2 (see Table 3). The ^{14}C activity of DIC in groundwater inflow was assumed to be very low (2 pmC). Only one measurement of ^{14}C activity of DIC in Rio Puerco water was available (64 pmC). Additional calculations were made in which the ^{14}C activity of DIC in Rio Puerco water was assumed to be 100 pmC, to represent possible conditions during times of high flow/runoff (see Plummer et al. 2004).

Values of $\delta^{13}C$ of DIC in source waters were assigned using logic similar to that used to assign ^{14}C activities. Consequently, $\delta^{13}C$ of DIC in mountain-front waters was set to a value of –12 per mil, which is that observed in modern mountain-front recharge. As discussed below, there may have been a higher abundance of C_4 plants in recharge areas of the MRGB in the past than today, resulting in $\delta^{13}C$ values of recharge waters more positive than that observed today ($\delta^{13}C$ of recharge near –8 per mil, historically). However, in all the geochemical models constructed, a $\delta^{13}C$ value of –12 per mil was used (Table 3) that is consistent with modern observations. Because the stable carbon isotopes were not used to constrain the geochemical reactions, the modeled mass transfers do not depend on the assumed initial value of $\delta^{13}C$ of DIC in recharge waters.

The possibility that many of the waters of the MRGB are mixtures of two or more source waters also was considered. Saline waters and, in some cases, unusually warm saline waters were sampled in a few localities in the basin; therefore, the potential for upward leakage of saline water also was considered in the models. Ranges and

 DOI 10.1007/s10040-004-0324-6

Table 3 Summary of chemical and isotopic properties of representative source waters for the Middle Rio Grande Basin. *Sevilleta*, [Moore 1999, Precipitation chemistry data on the Sevilleta National Wildlife Refuge, 1989–1995 (http://sevilleta.unm.edu/research/local/nutrient/precipitation/#data)]; PRECIPx8, Sevilleta with evapotranspiration (ET) factor of 8-fold; *NMF* northern mountain front, median; *EMF* eastern mountain front, median; *SWMF* southwestern mountain front, NWIS representative sample; *NEGW* northeast groundwater inflow, NWIS, representative sample; *SWGW* southwest groundwater inflow, NWIS, median; *ASSP* Arroyo Salado spring; *MWGW* mid-west groundwater inflow, NWIS, median; *Saline 1*, mineralized upward leakage from domestic well #04, NM041; *Saline 2* mineralized upward leakage from Coyote Spring, NM031; *RP* discharge-weighted average NWIS Rio Puerco at Bernardo; *RGA* discharge-weighted average NWIS Rio Grande at Albuquerque; *RGSF* discharge-weighted average NWIS Rio Grande at San Felipe; *JRW* discharge-weighted average NWIS Jemez River below Jemez Canyon Dam; *ABO* median Abo Arroyo; *TIJ* discharge-weighted average NWIS Tijeras Arroyo above Four Hills Road; *GAL* Galisteo Creek above reservoir, June 1974; *LUC* Lucero-24, Los Alamos National Laboratory, representative of southwest arroyo water; *NMxxx numbers* refer to sample numbers from Plummer et al. (2004); *Est.* estimated; *nd* no data

Source	pH	Est. dissolved oxygen	Alkalinity HCO_3^-	Calcium	Magnesium	Sodium	Potassium	Chloride	Sulfate	Silica	Est. $\delta^{13}C$	Est. ^{14}C activity
		(mg/L)	(mg/L)	(mg/L)	(mg/L)	(mg/L)	(mg/L)	(mg/L)	(mg/L)	SiO_2 (mg/L)	(per mil)	(pmC)
Precipitation												
Sevilleta (1989–1995) bulk	5.4	nd	1.7	0.94	0.09	0.12	0.15	0.21	1.40	nd	–8.0	100
Precipitation with ET of 8-fold												
PRECIPx8	5.4	8.0	0.525[a]	7.5	0.7	1.0	1.2	1.7	11.2	nd	–8.0	100
Mountain-front recharge												
NMF	7.4	8.0	124	29	3.9	16	4.3	4.4	14	53	–12.0	100
EMF	7.4	8.0	212	61	7.5	16	1.6	6.4	31	23	–12.0	100
SWMF	7.3	8.0	207	54	12.0	19	1.3	12.0	33	29	–12.0	100
Groundwater inflow												
NEGW	7.5	0.0	328	67	15.0	67	5.0	27.0	63	13	–4.0	2
SWGW	7.7	0.0	2,073	474	230	6,069	143	7,202	5,020	21	–4.0	2
ASSP	6.7	7.4	1,180	607	513	5,910	149	8,070	3,750	17	2.8	8
MWGW	7.7	0.0	1,366	300	145	3,532	117	2,700	3,250	21	–4.0	2
Upward leakage of saline waters												
Saline 1	7.0	0.1	182	185	26	1,530	107	2,520	296	43	–7.5	23
Saline 2	6.5	2.8	1,305	322	70	382	44	581	140	17	–0.6	5
Surface waters												
RP	8.0	1.0	183	138	29	200	7.0	46	707	10	–0.1	64
RGA	8.1	8.0	118	37	6.4	22	3.0	9.2	58	19	–7.5	100
RGSF	8.1	8.0	112	35	6.3	17	2.6	4.8	50	18	–7.5	100
JRW	8.1	8.0	129	39	4.6	62	5.5	50	79	22	–2.9	83
ABO	8.3	8.0	254	297	105	123	1.5	61	1,049	19	–7.1	87
TIJ	8.2	8.0	243	102	21	39	5.5	82	105	16	–7.1	87
GAL	8.1	8.8	220	150	45	140	3.7	23	630	17	–6.0	100
LUC	6.8	nd	536	171	57	131	5.4	46	183	18	–5.0	100

[a] mg/l as CO_2

DOI 10.1007/s10040-004-0324-6

averages of the percent contribution of each source water to a mixture are summarized for each sample in Plummer et al. (2004) and averaged for each hydrochemical zone in Table 4. The geochemical models indicate that most samples in the Northern Mountain Front, Northwestern, West-Central, Southwestern Mountain Front, and Eastern Mountain Front zones contain typically 98.5–100% mountain-front source water that has mixed generally with small fractions of saline upward leakage water. The fractions of "saline water 1" were lowest in the Northwestern and Southwestern zones and averaged 1.5, 0.7, and 1.0% in the Northern Mountain Front, West-Central, and Eastern Mountain Front zones, respectively. The source of saline water is attributed to upward leakage along faults.

The geochemical models indicate that water samples from the Western Boundary and Rio Puerco zones contain on average 7.8 and 7.4%, respectively, of saline groundwater inflow from sources along the western margin of the basin. Water samples in the Rio Puerco zone contain an average of 92.6% Rio Puerco water. Water from the Western Boundary zone averages about 92% water from local arroyo recharge along the western boundary of the basin. Water samples from the Abo Arroyo zone predominantly were of eastern mountain front origin mixed with an average of 28% Abo Arroyo water. Water from the Central zone was almost entirely of Rio Grande origin, averaging 99.6% water of Rio Grande origin (range 96.5–100%), which was mixed with "saline water 1". Waters from the Tijeras Fault Zone and Tijeras Arroyo zones were found to be fairly complex mixtures of eastern mountain front water with varying fractions of Tijeras Arroyo water and "saline waters 1 and 2". Waters in the Northeastern zone apparently are complex mixtures of eastern mountain front water, northeast groundwater inflow, surface water from Galisteo Creek, and "saline water 1" (Table 4). The geochemical mass-transfer calculations indicate that there is net evaporation (evapotranspiration) throughout most of the MRGB, except in the Western Boundary and Eastern Mountain Front zones, where overall dilution (modeled with pure water) is indicated (Table 5).

Average values of mineral mass transfer, in mmol kg^{-1} water, and the average calculated evaporation factor are summarized in Table 5 for each hydrochemical zone. The calculated average mass transfers generally are quite small, yet there probably is some significance to the differences in values between hydrochemical zones. The NETPATH models indicate that, on average, there is net precipitation of small amounts of calcite through most of the MRGB. The exception is the West-Central zone, where the calculations indicate that small amounts of calcite dissolve in association with small relative increases in Ca/Na cation exchange. The net calcite mass transfer is near zero in other parts of the basin (Northern Mountain Front, Northwestern, and Central zones). Small amounts of plagioclase feldspar weathering were observed throughout the MRGB. Small masses of kaolinite, and probably other clay minerals, form throughout the ba-

Table 4 Summary of predominant groundwater sources by hydrochemical zone. *NMF* western mountain front, NWIS; *EMF* eastern mountain front, median; *ABO* median Abo Northern mountain front; *Saline 1* NM041; *RP* discharge-weighted average NWIS Rio Arroyo; *Saline 2* Coyote Spring, NM029; *TIJ* discharge-weighted average NWIS Tijeras Puerco; *RGA* discharge-weighted average NWIS Rio Grande at Albuquerque; *MWGW* Arroyo; *NEGW* northeast ground water inflow; *GAL* Galesteo Creek above reservoir, used mid-west ground-water inflow; *SWGW* southwestern ground-water inflow; *SWMF* south- as arroyo source in hydrochemical zone 11

Zone no.	Hydrochemical zone	Primary water	Percent range of primary water	Average percent of primary water	Secondary water 1	Percent range of secondary water 1	Average percent of secondary water 1	Secondary water 2	Percent range of secondary water 2	Average percent of secondary water 2
1	Northern Mountain Front	NMF	92.3–100	98.5	Saline 1	0–7.3	1.5			
2	Northwestern	NMF	97.1–100	99.9	Saline 1	0–2.9	0.1			
3	West Central	NMF	92.5–100	99.3	Saline 1	0–7.5	0.7			
4	Western Boundary	LUC	84.0–100	92.2	ASSP	0–16.0	7.8			
5	Rio Puerco	RP	77.6–100	92.6	MWGS or SWGW	0–22.4	7.4			
6	Southwestern Mountain Front	SWMF	100	100.0	Saline 1	0	0.0			
7	Abo Arroyo	EMF	47.7–100	72.1	ABO	0–52.3	27.9			
8	Eastern Mountain Front	EMF	89.5–100	99.0	Saline 1	0–10.5	1.0			
9	Tijeras Fault Zone	EMF	61.2–100	89.5	Saline 1,2	0–38.8	10.5			
10	Tijeras Arroyo	EMF	2.9–92.3	61.6	TIJ	9.1–91.6	37.4	Saline 2	0–6.6	1.6
11	Northeastern	EMF	14.2–98.9	66.3	NEGW, GAL	1.1–85.8	33.4	Saline 1	0–2.0	0.3
12	Central	RGA	96.5–100	99.6	Saline 1	0–3.5	0.4			

DOI 10.1007/s10040-004-0324-6

Table 5 Summary of average mineral mass transfers and evapotranspiration/dilution factor by hydrochemical zone. *CH_2O* Organic carbon; evapotranspiration/dilution factor >1 for evaporation, <1 for dilution; mineral mass transfer negative for precipitation (outgassing), positive for dissolution

Zone no.	Hydrochemical zone	Average mass transfer (mmol kg^{-1} water)								Evaporation/ dilution factor
		Calcite	Plagioclase	CO_2	Kaolinite	SiO_2	Ca–Na exchange	Gypsum	CH_2O	
1	Northern Mountain Front	0.06	0.27	1.15	–0.19	–0.24	–0.16	0.14	nd	1.06
2	Northwestern	0.06	0.01	0.00	–0.01	0.00	0.84	0.27	nd	1.06
3	West Central	0.39	0.07	0.31	–0.05	–0.44	1.80	0.93	nd	1.15
4	Western Boundary	–3.98	0.11	–0.18	–0.07	0.27	2.92	7.32	nd	0.67
5	Rio Puerco	–1.96	0.18	1.43	–0.12	0.16	–3.19	1.19	nd	1.21
6	Southwestern Mountain Front	–0.97	0.07	–1.21	–0.05	–0.48	0.00	0.04	nd	2.19
7	Abo Arroyo	–0.75	0.09	–0.62	–0.06	–0.10	–0.02	–0.36	nd	3.41
8	Eastern Mountain Front	–0.26	0.34	0.43	–0.23	–0.18	0.14	0.22	nd	0.86
9	Tijeras Fault Zone	–0.83	0.59	–0.11	–0.41	–0.78	–0.28	0.59	nd	2.13
10	Tijeras Arroyo	–0.86	0.20	0.00	–0.14	–0.24	–0.09	0.70	nd	1.13
11	Northeastern	–1.23	0.60	–0.20	–0.41	–0.67	0.42	1.57	nd	1.51
12	Central	0.00	0.18	0.12	–0.12	0.22	0.08	–0.10	0.28	1.34

sin as primary aluminosilicate minerals, such as plagioclase feldspars dissolve.

Additional sources of carbon included CO_2 gas and organic matter (CH_2O). The CO_2 mass transfer is expected to be small because most groundwater systems are closed to gas exchange after recharge. Although the calculated CO_2 mass transfers are not zero, they are small and reflect, in part, uncertainties in the DIC content of paleo-recharge waters, and small analytical errors that NETPATH ultimately compensates for in the calculated masses of phases such as CO_2 and CH_2O, which are not formed by combining charged constituents. Cation exchange appears to be relatively important in the Northwestern, West-Central, Western Boundary, and Northeastern zones. Gypsum abundance is low or zero throughout most of the MRGB sediment, except in parts of the Western Boundary and Rio Puerco zones, where the calculated mass of gypsum dissolution is higher than in other hydrochemical zones. The small differences in gypsum mass transfer outside of the Western Boundary and Rio Puerco zones probably reflect, at least in part, uncertainty in the calcium sulfate content of source waters to the MRGB. Redox reactions were considered only in the Central zone, where there are anoxic conditions in the inner valley of the Rio Grande. Here, the NETPATH models found, on average, a net oxidation of 0.28 mmol kg^{-1} of organic carbon. Calculations in which carbon-isotopes exchange between calcite and DIC lead to impossibly young (negative ages) radiocarbon ages in many cases. Therefore, carbon isotope exchange likely is not an important process in the predominantly siliciclastic sediment of the MRGB.

Radiocarbon Ages

In most cases, the adjusted radiocarbon age was nearly identical to the unadjusted radiocarbon age, indicating that geochemical reactions do not appreciably affect the calculated ages. For hydrochemical zones 1–12, respectively, the average differences in unadjusted and adjusted radiocarbon ages (both ages calculated using the Libby half-life) are 0.5, 1.2, 1.0, 1.2, 4.9, -0.1, 0.2, 0.1, 3.7, 1.3, 2.5, and 0.3 ka, respectively. The largest differences between unadjusted and adjusted radiocarbon ages occur for some waters from hydrochemical zones 5, 9, and 11, and result from mixing with relatively large fractions of old groundwater with low ^{14}C activity, rather than the result of water-rock reaction. Most of the samples from hydrochemical zones 1–4, 6–8, 10, and 12 have adjusted ages that are nearly identical to the unadjusted age because the geochemical mass transfers are small and the samples contain relatively small fractions of old groundwater inflow or old saline sources. Sensitivity calculations, in which compositions of clays, feldspars, and ion exchangers were varied within reasonable limits, did not appreciably alter adjusted ^{14}C ages. Details of the NETPATH model results are given for each water sample from the MRGB in Plummer et al. (2004), and are summarized for each hydrochemical zone in Tables 4 and 5.

The evaluation using NETPATH is far from exhaustive, but shows that the extent of geochemical reactions affecting the chemical and isotopic composition of waters in the MRGB probably is small and generally has negligible effect on the initial ^{14}C activity, A_o. Although the reaction modeling is non-unique, any other reactions that might affect the waters of the MRGB also are thought not to significantly affect the initial ^{14}C activity. Therefore, the unadjusted radiocarbon age was adopted in the present investigation.

 DOI 10.1007/s10040-004-0324-6

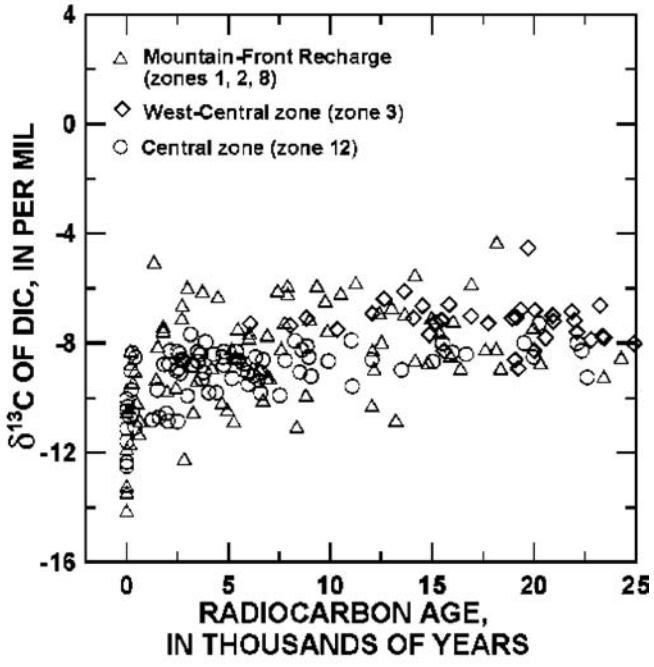

Fig. 10 $\delta^{13}C$ isotopic composition of dissolved inorganic carbon as a function of radiocarbon age for waters from basin margins (hydrochemical zones 1, 2, and 8), the West-Central zone (zone 3), and the Central zone (zone 12)

Carbon-13 Isotopic Composition of Dissolved Inorganic Carbon

There is generally little variation in HCO_3 concentration or $\delta^{13}C$ composition of DIC within a particular hydrochemical zone. Of the 195 values of $\delta^{13}C$ of DIC in groundwater from the MRGB for which the radiocarbon age is greater than 200 years (Fig. 10), $\delta^{13}C$ of DIC averages –8.2±1.4 per mil. The lack of variation in $\delta^{13}C$ and HCO_3 concentration within a hydrochemical zone indicates that geochemical reactions involving carbon are probably limited in the aquifer system. This observation was also supported by the NETPATH calculations that indicated negligible effect of the geochemical reactions on the $\delta^{13}C$ of the primary source water. Apparently, $\delta^{13}C$ of the DIC in recharge waters to the MRGB has been remarkably constant for most of the past 25 ka (Fig. 10).

Although the data are limited, seven groundwater samples from remote areas of the Northern and Eastern Mountain Front zones with radiocarbon ages less than 200 years are depleted in ^{13}C relative to most samples within the basin, and average –11.9±2.0 per mil. Today, and in the very recent past (perhaps as recently as only the past 200 years), $\delta^{13}C$ of DIC in recharge waters along the basin margins apparently has become depleted in ^{13}C, by about 4 per mil, relative to a value of about –8.2 per mil that prevailed for the previous 25,000 years. No geochemical reactions were found using NETPATH that would account for an increase of 4 per mil in $\delta^{13}C$ between post-bomb and pre-bomb waters along the basin margins. Young groundwater of Rio Grande origin (Fig. 10) also indicates a fairly recent decrease in $\delta^{13}C$ of DIC, relative to older water of Rio Grande origin.

Measurements of $\delta^{13}C$ of pedogenic carbonates in southern Arizona indicate C_4 plant dominance during the last glacial period, followed by a decrease that has been attributed to a replacement of C_4 grasslands during the Holocene by C_3/CAM desert shrubs and succulents (Liu et al. 1996). Liu et al. (1996) attributed the replacement to climatic factors including an increase in temperature and reduction in summer precipitation at the end of the last glacial period. The landscape in southern Arizona apparently was predominantly C_4 grasslands for most of the past 700 ka (Liu et al. 1996).

Eleven specimens of caliche from soils and drill cuttings from throughout the basin had $\delta^{13}C$ values of –4.3±0.9 per mil, which compares to an average $\delta^{13}C$ value of –0.9±1.9 per mil for ten samples of Pennsylvanian limestones that cap the Sandia and Manzano Mountains on the east side of the basin. Three of the eleven caliche samples were radiocarbon dated and had $\delta^{13}C$ val-ues of –2.9, –3.8, and –5.3 per mil, with Conventional Radiocarbon Ages of 27.4, 7.2, and 2.3 ka B.P., respectively. The isotopic values for the three samples of caliche are consistent with a possible decrease in the proportion of C_4 plants in late Holocene ecosystems (Grover and Musick 1990; Liu et al. 1996), but on a time-scale of perhaps 7 ka.

The $\delta^{13}C$ values from the MRGB (–8.2±1.4 per mil) are considerably more enriched in ^{13}C than those reported by Phillips et al. (1989) for waters in the San Juan Basin, in northwest New Mexico (average $\delta^{13}C$ of –14.1±3.4 per mil). From studies of $\delta^{13}C$ of herbivore tooth enamel, Connin et al. (1998) found that during the last glacial period there was a significant increase in C_4 plant abundance eastward across the southwestern United States, which may, in part account for the differences between the $\delta^{13}C$ values of the San Juan Basin and MRGB. Using modern correlations between climate and C_4 grass abundance, Connin et al. (1998) concluded that there was significant summer precipitation in parts of southern Arizona and New Mexico during the last glaciation.

The data presented here indicate that C_4 plant dominance prevailed in the MRGB through the last glacial period and through most of the Holocene. The increase in C_3 plant abundance in the MRGB may be a relatively recent phenomena, as has been observed in southern New Mexico (Grover and Musick 1990; Monger et al. 1998), parts of southeastern Arizona (McPherson et al. 1993), and along the Rio Grande Plains of southern Texas, where measurements of $\delta^{13}C$ and ^{14}C activity of soil organic carbon indicate that a shift from C_4 grassland to C_3 woodland occurred as recently as the past 50 to 100 years (Boutton et al. 1998).

Apparently, a number of factors including amount and seasonality of precipitation, temperature, soil texture, and atmospheric P_{CO2} can influence the relative abundances of C_3 and C_4 plants (Epstein et al. 1997; Huang et al. 2001). Regardless of the processes responsible for determining the $\delta^{13}C$ of DIC recharged to the MRGB, the groundwater chemistry provides evidence of recharge of DIC to the

 DOI 10.1007/s10040-004-0324-6

MRGB that has been relatively enriched in ^{13}C throughout most of the past 25 ka, and has been mostly unaffected by geochemical reactions in the aquifer system.

Radiocarbon Calibration

Because the radiocarbon ages in the MRGB are mostly insensitive to the recharge and reaction processes that can often obscure radiocarbon dating in carbonate aquifers, it was concluded that the radiocarbon ages in the MRGB may be accurate enough to warrant further conversion to calendar years, taking advantage of recent compilations and extensions of radiocarbon calibration data. Radiocarbon calibration scales are needed because the strength of the Earth's geomagnetic field has varied over time and, consequently, the ^{14}C activity of atmospheric CO_2 has varied in the past, and for the most part has been somewhat greater than 100 pmC (Stuiver et al. 1986; Bard et al. 1990, 1993; Stuiver and Reimer 1993; Bartlein et al. 1995). The conversion to calendar years is still a relatively small refinement for hydrologic systems, but probably provides more accurate estimates of calendar ages and travel times for use in calibration of a groundwater-flow model (Sanford et al. 2004a, 2004b).

Radiocarbon calibration data from various sources (Bard et al. 1998; Kitagawa and van der Plicht 1998a, 1998b, 2000; Stuiver et al. 1998) gives the correction that is added to the apparent unadjusted radiocarbon age (Libby half-life) to correct to calendar years (Plummer et al. 2004; Fig. 11). Over the range of most of the unadjusted radiocarbon ages of the waters in the MRGB, the calendar-year age differs from the unadjusted radiocarbon age between 0 and about 3 ka. Waters from the Tijeras Arroyo and Central zones have median unadjusted radiocarbon ages of approximately 5 ka and for these, the average calendar age is less than 1 ka greater than the unadjusted radiocarbon ages (Fig. 11). Water from the Northern Mountain Front, Northwestern, Rio Puerco, Southwestern Mountain Front, Abo Arroyo, Eastern Mountain Front, and Tijeras Fault Zone zones has, on average, calendar-year ages that are about 1 ka greater than the apparent unadjusted radiocarbon age (Fig. 11). The oldest waters sampled in the MRGB, from the West-Central and Western Boundary zones, have unadjusted calendar-year ages that are typically 3 ka older than the unadjusted radiocarbon ages (Fig. 11).

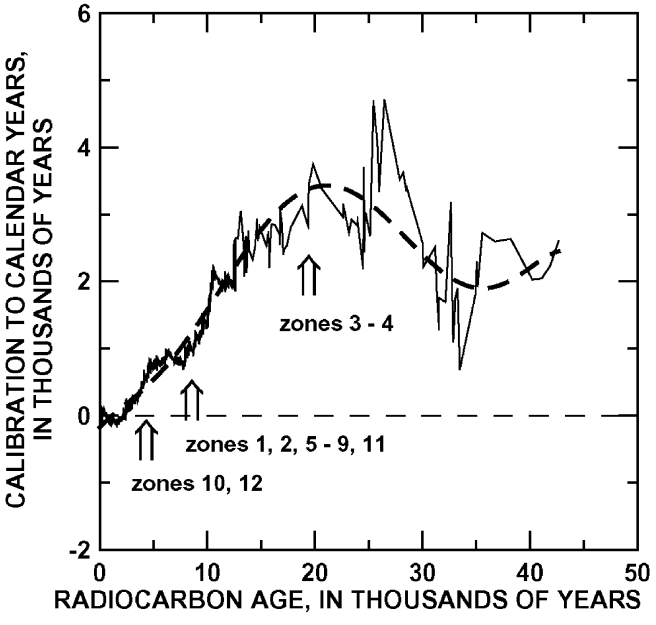

Fig. 11 Summary of radiocarbon calibration data from various sources (see text). The *curve* shows the correction to be added to the unadjusted radiocarbon age to correct to calendar years; however, all radiocarbon ages reported in this study are the unadjusted radiocarbon age (Libby half-life). Hydrochemical zone numbers are identified in Tables 4 and 5. For most waters of the MRGB, the correction is less than 1 ka. For waters from zones 3 and 4, the calendar-year ages are, on average, about 3 ka greater than the unadjusted radiocarbon age

Regional Variations in Radiocarbon Age

Ages Near the Water Table

The unadjusted radiocarbon age of water in the upper approximately 60 m of the Santa Fe Group aquifer system throughout the MRGB is shown in Fig. 12. The youngest water (0–2 ka) is along the mountain-front basin margins (eastern edge of the Eastern Mountain Front zone, the northeast, northwest, and southwest margins of the basin), and along parts of the Rio Grande and Rio Puerco. Water with DIC unadjusted radiocarbon age of 0–10 ka extends along nearly the entire reach of the Rio Grande, the Rio Puerco, Galisteo Creek, Tijeras Arroyo, and Abo Arroyo, and is associated with relatively recent surface-water infiltration. The oldest waters are at the water table through the West-Central zone, the Western Boundary zone, and parts of the Eastern Mountain Front zone, and throughout the Discharge zone (Fig. 12). The old age of water near the water table indicates that there has been little or no direct infiltration of precipitation over large areas of the MRGB during at least the past 20–30 ka.

The median unadjusted radiocarbon age of DIC in groundwater from 275 analyses throughout the MRGB, excluding samples contaminated with post-bomb ^{14}C, is 8.1 ka, with a range of ~0–>30 ka. In the mountain-front hydrochemical zones, the median unadjusted radiocarbon age is, for the Northern Mountain Front, Northwestern, Southwestern, and Eastern Mountain Front zones, 8.8, 8.8, 7.7, and 5.2 ka, respectively. Water in the West-Central, Western Boundary, and Discharge zones is relatively old, with median unadjusted radiocarbon ages of 19.5 20.4, and 17.9 ka, respectively. Groundwater dominated by river/arroyo sources has median unadjusted radiocarbon ages of 8.1, 4.6, and 3.2 ka for the Rio Puerco, Central, and Tijeras Arroyo zones, respectively. The median unadjusted radiocarbon ages of DIC in water from the Abo Arroyo, Tijeras Fault Zone, and Northeastern zones are 9.4, 16.2, and 10.0 ka, respectively.

 DOI 10.1007/s10040-004-0324-6

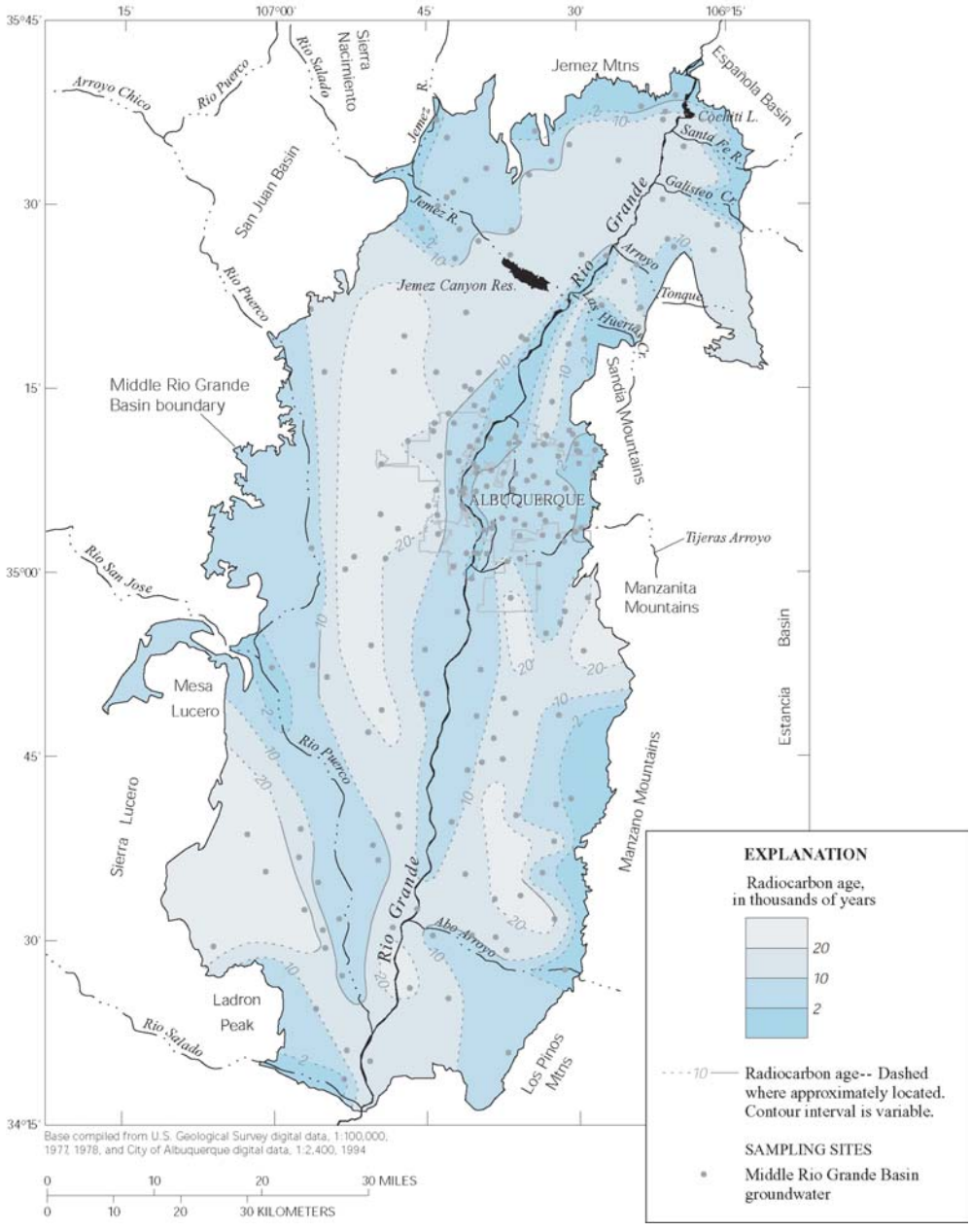

Fig. 12 Regional variations in the unadjusted radiocarbon age of DIC in groundwater from approximately the uppermost 60 m of the aquifer system, Middle Rio Grande Basin

Age Gradients

Additional data are available describing radiocarbon age as a function of depth in various parts of the MRGB. Although water composition and stable isotopic composition are relatively constant to depths of more than 200 m in the MRGB, there can be appreciable variation in groundwater age with depth. The most reliable age information as a function of depth was obtained from the piezometer nests that are open to relatively narrow intervals (typically 1.5–3 m) of the aquifer system (Fig. 13). The average age gradient, expressed as years per cm of aquifer (year cm^{-1}), was calculated between the upper- and bottom-most interval from the piezometer nests that extend over 70 to more than 400 m of the aquifer system. The average age gradient from this set of piezometer nests is 0.6±0.4 year cm^{-1}. The average age between the upper and lowest interval is 12.2±6.1 ka.

There are differences in the magnitude of age gradients depending on many factors, including location and average age. Some of the smallest age gradients (equal to relatively large thicknesses of water of similar age) were calculated between the upper- and bottom-most interval along the eastern mountain front (Eastern Mountain Front zone), such as at well nest S114–S116 (0.23 year cm^{-1} with a mean age of 6.9 ka); along the west side of the Rio Grande north of Albuquerque (Central zone), at nest S075–S078 (0.25 year cm^{-1}, mean age of 6.7 ka); and between nests S004–S006 (mostly West-Central zone; 0.22 year cm^{-1}, mean age of 24.3 ka). Age gradients in the

 DOI 10.1007/s10040-004-0324-6

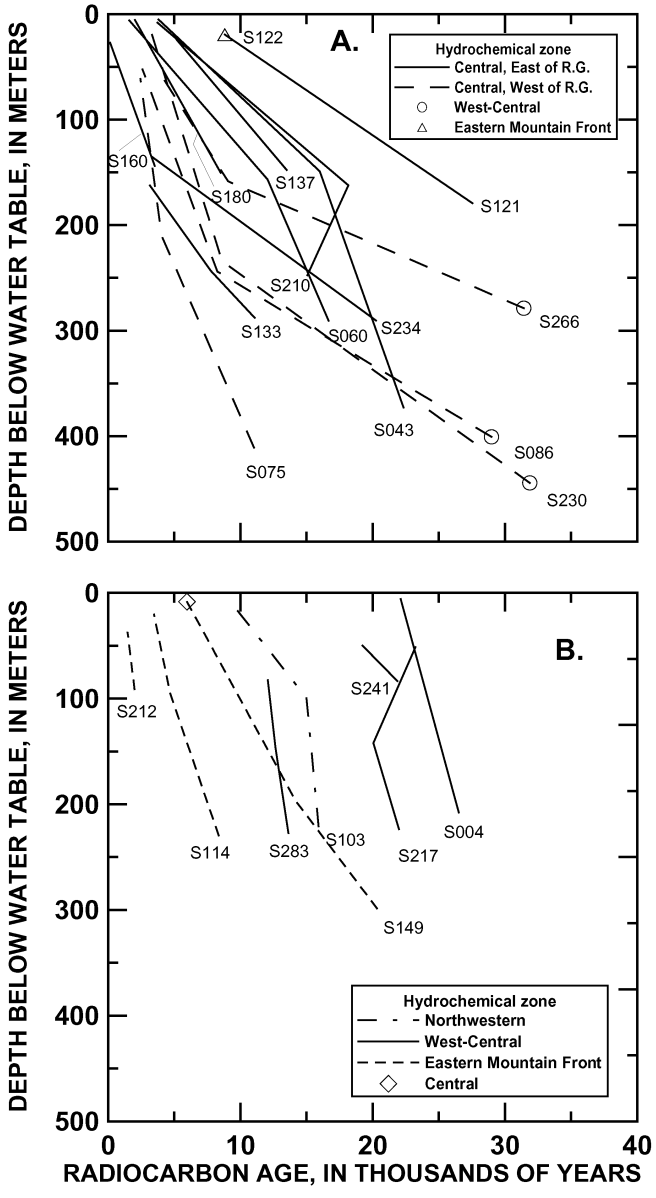

Fig. 13 A, B Profiles of radiocarbon age as a function of depth from piezometer nests from the Middle Rio Grande Basin. **A** Piezometer nests penetrating waters of the Central hydrochemical zone, either east or west or the Rio Grande. *Symbols* denote piezometer nests where the deep completion is in the West-Central zone or the shallow completion is in the Eastern Mountain Front zone. **B** Piezometer nests in the Northwestern, West-Central and Eastern Mountain Front zones. Water at the shallow completion of the piezometer nest in the Eastern Mountain Front zone at site S149 is of Rio Grande origin (Central zone). The piezometer locations are shown on Figs. 3 and 5

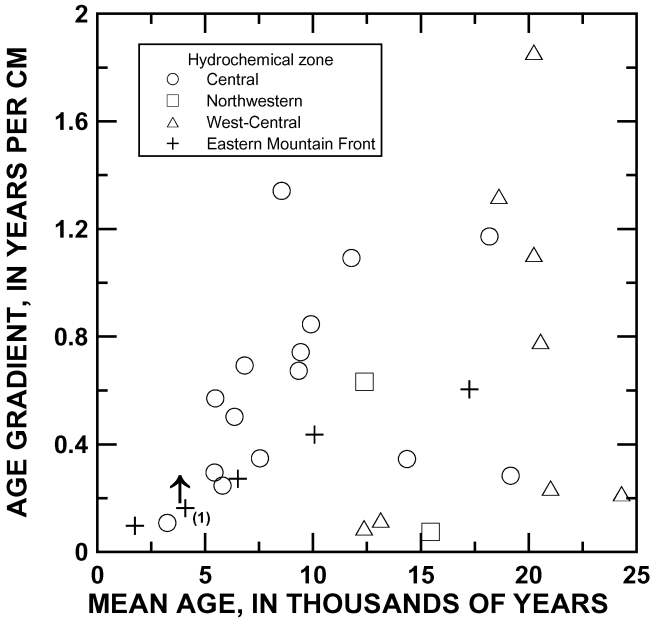

Fig. 14 Age gradients in years per centimeter (year cm^{-1}) of aquifer calculated between each pair of open intervals for each piezometer nest and plotted at the mean radiocarbon age of the two intervals. Age gradients vary from about 0.1 to 2 year cm^{-1} of aquifer in the upper 600 m of aquifer and are quite variable for waters older than about 10 ka. Relatively low age gradients are found for waters recharged in the past 5 ka. (1) S115–S116 mid-shallow interval. Water-level measurements indicate that water at the shallow depth of piezometer S116 is perched, resulting in likely under-estimation of the age gradient between the mid- and shallow depths at this piezometer

upper 250 m of the Central zone along the west side of the Rio Grande are lower than on the east side of the Rio Grande. However, below 250 m, age gradients in the Central zone tend to be higher west of the Rio Grande than observed east of the Rio Grande (Fig. 13A).

Most age gradients do not extrapolate to zero age at the water table (Fig. 13), indicating that groundwater in the piezometer nest likely has moved horizontally from the point of recharge, and that following recharge and flow to the present location, little or no additional water has been added to the water table for periods as long as 20 ka (S004, Fig. 13B). The piezometer nests from the Eastern Mountain Front zone (Fig. 13B) that extrapolate nearest to zero age at the water table (S212 and S114) are located adjacent to the eastern mountain front at Albuquerque.

More detailed age-depth information is found by calculating age gradients between each depth interval for each piezometer nest. Typically, two values are calculated for each nest, between the deep and medium completions and the medium and shallow completions. Several piezometer nests have four completions, yielding three values of the age gradient at those locations. The resulting age gradients, calculated between each pair of open intervals, vary between about 0.1 and 2 year cm^{-1} (Fig. 14). During the past 15 ka, the piezometer nests indicate a maximum age gradient at about 10 ka and minimum between about 12–16 ka. The age gradients (in year cm^{-1}) tend to decrease from a maximum at 10 ka to relatively low values during the past few thousand years (Fig. 14). Higher age gradients generally are found between the deep and medium completions than between the medium and shallow completions. The age gradients from two piezometers in the youngest (and most shallow) waters along the Eastern Mountain Front and the Central zone are about 0.1 year cm^{-1} (Fig. 14). The implied modern

 DOI 10.1007/s10040-004-0324-6

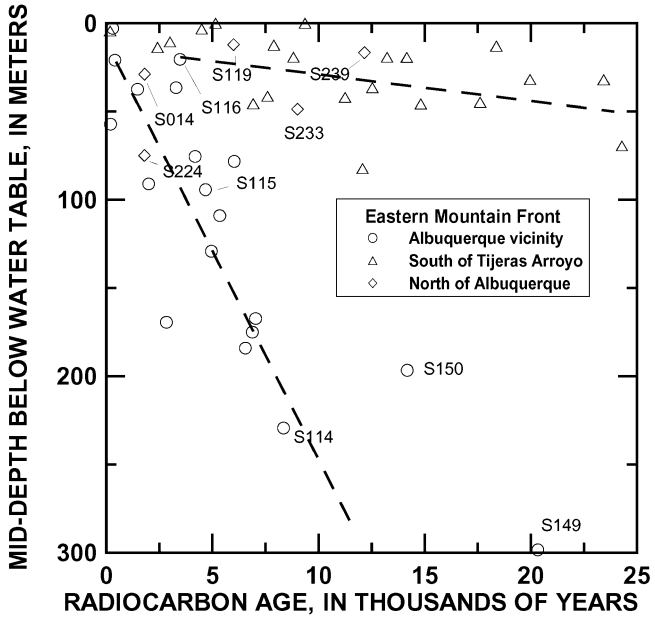

Fig. 15 Radiocarbon age as a function of the depth below the water table of the mid-point of the open interval for all wells from the Eastern Mountain Front zone. Two age depth relations are apparent. A relatively thick zone of recharge from the eastern mountain front is observed at Albuquerque, but in areas north of Albuquerque and south of Tijeras Arroyo, there has been relatively less recharge of comparable age to the Eastern Mountain Front zone. Locations of selected wells are shown on Figs. 3 and 5

recharge rate near the eastern mountain front and Rio Grande from these two piezometers is on the order of 3 cm year^{-1}, assuming an average porosity of 0.3, and is within the range of recharge rates reported for other semiarid environments (see for example, Scanlon et al. 2002; Flint et al. 2002; Zhu et al. 2003). Although there is an appearance of temporal variation in age gradients, it can be ambiguous to examine age gradients out of context for the groundwater flow system. Furthermore, flow in recharge areas is not vertical at any of the piezometer nests, and some nests are near discharge areas. For example, in the period 15–25 ka, age gradients vary by a factor of nearly 20 (Fig. 14).

Along the eastern mountain front, there appear to be two different age–depth relations. In the calculations of Fig. 15, radiocarbon ages for all samples from wells in the Eastern Mountain Front zone (production, domestic, and monitoring wells) were used and age was plotted at the mid-depth of the open interval in meters below the water table. Water from the Eastern Mountain Front zone found north of Albuquerque, or south of Tijeras Arroyo, has a relatively high age gradient (~6.6 year cm^{-1}) in relation to waters from the Eastern Mountain Front zone at Albuquerque (~0.4 year cm^{-1}; Fig. 15). Apparently, over at least the past 10 ka, there has been appreciably more recharge along the eastern mountain front at Albuquerque than either to the north or south of the Albuquerque vicinity. Factors that may contribute to this difference are a greater thickness of ancestral Rio Grande sands at Albuquerque than elsewhere along the eastern mountain front (Hawley and Haase 1992), the presence of the Hubble Bench and Tijeras and Hubble Springs fault zones to the south, which place low permeability rocks at shallow depths, and higher precipitation rates along the Sandia Mountains at Albuquerque than along lower altitude portions of the eastern mountain front.

Because of the relatively high density of wells and piezometer nests in the vicinity of Albuquerque, it is possible to construct cross sections through the upper 600 m of the aquifer system showing age relations and stable isotope composition in relation to hydrochemical zones. One such cross section (Hawley 1996b), constructed approximately east–west and aligned along Menaul Blvd. through central Albuquerque (Fig. 16), shows the extent and age of water of Rio Grande origin beneath Albuquerque in relation to waters from the West-Central and Eastern Mountain Front zones. Isotopically depleted water of radiocarbon age more than 20 ka is found at the water table west of the Rio Grande and at depth beneath Central zone waters under the inner valley of the Rio Grande. Relatively young water of Rio-Grande-origin flows south along the contact with paleo-water of the West-Central zone (Fig. 16). There are relatively sharp boundaries between hydrochemical zones.

Although there is considerable age–depth information available for the waters of the MRGB (Plummer et al. 2004), computed inventories of water volumes of different ages were highly uncertain due to lack of information on age gradients with depth over large parts of the basin. Attempts to estimate recharge rates from estimates of water volumes as a function of age were even more uncertain due to inability to account for volumes of water that have already discharged from the basin. It was concluded that the most reliable estimates of recharge rate that can be derived using the radiocarbon ages from this study are obtained when the radiocarbon ages are used in conjunction with the calibration of a basin-scale groundwater-flow model (Sanford et al. 2004a, 2004b).

Implications from Geochemical and Isotopic Data for the Conceptual Model of the Groundwater System

Tracing Sources of Water Through the Basin

In most cases, groundwater that has separate recharge sources differed in major-/minor-element chemistry and isotopic composition. In other cases, the use of isotopic data, particularly ^{2}H and ^{14}C, was essential to differentiating waters of separate origin. The study shows that because the siliciclastic sediments of the Santa Fe Group aquifer system are relatively unreactive, the chemical composition of groundwater in the basin generally changes little along a flow path, permitting source waters to be traced over long distances through the aquifer system.

Mountain-front recharge sources dominate over large areas along the northern and eastern margins of the basin, and in the southwest corner, and can be distinguished

 DOI 10.1007/s10040-004-0324-6

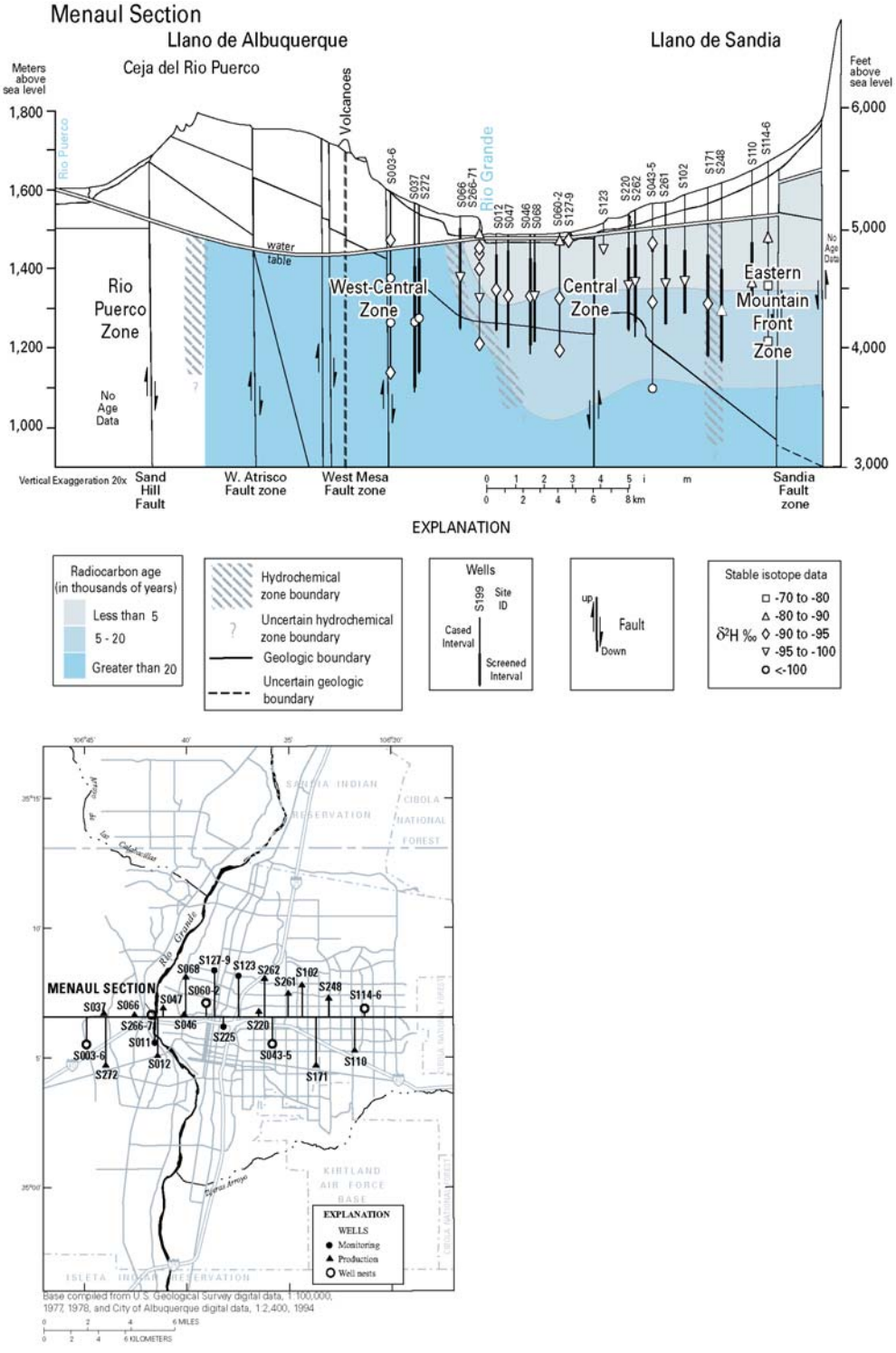

Fig. 16 Schematic hydrogeologic cross section of the Middle Rio Grande Basin, New Mexico, aligned with Menaul Boulevard, through central Albuquerque (based on Hawley 1996b), showing ranges of δ^2H and radiocarbon age for ground water in relation to position of hydrochemical zone boundaries. The location of the east–west cross section and well locations are shown on the adjacent map. The geologic boundaries are defined in Plummer et al. 2004)

from waters of the West-Central zone on the basis of chemical and isotopic composition (Tables 1 and 2). Infiltration from the Rio Grande, particularly in the area of Albuquerque, is another important source of recharge to the aquifer system of the MRGB. This study has helped to define the extent and age of water sourced at the Rio Grande (Fig. 8). The study indicates that water has been entering the aquifer system from the Rio Grande for tens of thousands of years and historically has flowed primarily north to south under the Albuquerque area (Figs. 5, 7, 8, and 16). Other sources of water to the basin are delineated on Fig. 8.

 DOI 10.1007/s10040-004-0324-6

Direction of Groundwater Flow

Conservative geochemical tracers and boundaries between hydrochemical zones indicate that groundwater flow in the MRGB historically has been directed primarily north–south through the center of the basin, with a greater east–west component near the basin margins.

Although predevelopment hydraulic-head maps for the MRGB (Bjorklund and Maxwell 1961; Titus 1961; Bexfield and Anderholm 2000; Fig. 2) are broadly consistent with the primary direction of groundwater flow indicated by geochemical data, there are some apparent inconsistencies. In particular, predevelopment hydraulic heads indicate greater east–west components of flow through the center of the basin than is suggested by the orientation of the hydrochemical zones. The differences in flow direction indicated by hydraulic heads compared to geochemical tracers likely are associated with the different time horizons and depths represented by the two types of information.

Carbon-14 data from this study of the MRGB indicate that most groundwater resides in the aquifer system for thousands to tens of thousands of years. Therefore, the hydrochemical zones defined on the basis of current groundwater chemistry in the basin probably reflect aquifer system conditions (including groundwater-flow directions) existing on the order of tens of thousands of years into the past, and may not yet reflect the "current" hydraulic-head distribution. In addition, predevelopment hydraulic-head maps for the basin were based on conditions primarily in the shallow part of the aquifer system (to a depth of at most 60 m), whereas geochemical data include samples collected from wells reaching greater depths, where groundwater flow directions may differ somewhat.

Origin of the Groundwater Trough

The predevelopment hydraulic-head maps of Titus (1961), Bjorklund and Maxwell (1961), and Bexfield and Anderholm (2000) have all indicated the existence of a groundwater trough in the western part of the MRGB, extending from near the Jemez River on the north to Belen on the south, and from a series of major faults on the west to near the Rio Grande on the east (Fig. 2). Water levels in the trough can be as much as 15 m lower than the level of the Rio Grande directly to the east. Geochemical data from this study show that groundwater flowing along the axis of the trough is within the West-Central hydrochemical zone and originated in the area of the Jemez Mountains during the last glacial period. Although hydraulic heads indicate that water sourced at the western margin of the basin and at the Rio Grande should be flowing into the center of the trough, the geochemical data indicate that the western margin and Rio Grande waters have not yet reached the center of the trough. The lack of evidence that these waters have reached the axis of the trough appears to contradict one conceptual model that the trough exists primarily as the result of a large thickness of relatively permeable materials near its axis that would cause the area to act as a sort of "drain" for the groundwater system (Kernodle et al. 1995). Recent geohydrologic data for the area do not support this conclusion (Hawley 1996b).

One possible explanation for the existence of the trough that would be consistent with the observed geochemical data is that the trough is a transient feature of the groundwater system in the MRGB. As mentioned above, changes with time in the quantity and distribution of recharge around the basin could result in a change in the distribution of hydraulic head. If the trough is a relatively recent (perhaps from the beginning of the Holocene) feature of the aquifer system, water sourced at the western margin of the basin and at the Rio Grande may not yet have had time to travel into the trough area. Radiocarbon ages of waters sourced from the western margin that are located today on the west side of the trough, and Rio Grande waters located on the east side of the trough, are approximately 10 ka (Fig. 12), and are younger than 10 ka further to the west and east toward the Rio Puerco and Rio Grande sources, respectively. This suggests that water has been flowing toward the trough from the Rio Puerco and Rio Grande since the beginning of the Holocene. Using a groundwater-flow model for the MRGB, Sanford et al. (1998) found that the trough could be simulated merely by lowering the quantities of recharge from the basin margins.

Other factors that could contribute to the presence of the trough could be horizontal anisotropy and the existence of features that limit groundwater flow into the trough from the east and west. Such features could include major faults that are relatively impermeable or low-conductivity geologic strata (McAda and Barroll 2002). Most major faults within the MRGB trend north to south; therefore, cementation of any of several major faults could be consistent with the restriction of east–west groundwater flow. Such restrictions would act only to limit flow toward the trough and not to prevent it entirely. Therefore, even if flow restrictions are important, the absence of water sourced from the Rio Grande and from the western margin near the axis of trough implies that the trough is a transient rather than a long-term feature.

Groundwater Flow in Relation to Faults

In the MRGB, a few boundaries between hydrochemical zones appear to correspond fairly closely in places with "major" faults identified by Mark Hudson and Scott Minor (US Geological Survey, written communication 1999). Two examples are the boundary between the Rio Puerco and West-Central zones and the boundary between the Tijeras Fault Zone and Eastern Mountain Front zones. The general correspondence of differences in groundwater chemistry with particular fault locations may indicate that horizontal groundwater flow is limited across those faults (Fig. 2).

Whereas there are differences in groundwater chemistry across sections of some "major" faults, differences in chemistry are not evident in other areas where impor-

 DOI 10.1007/s10040-004-0324-6

tant — even basin-bounding — faults exist. For example, the water-level map of Bexfield and Anderholm (2000) indicates the existence of a hydraulic discontinuity along the Sandia Fault adjacent to the front of the Sandia Mountains. However, the chemical and isotopic data indicate that the distinct chemical boundary between water sourced from the Rio Grande and water sourced along the eastern mountain front (Fig. 5) is approximately 3 km west of the Sandia Fault and apparently is unrelated to the location of the fault. The hydraulic discontinuity in this area (Fig. 2) probably is the result of the greater saturated thickness of conductive materials on the west side of the fault, resulting in a flatter hydraulic gradient on that side. Therefore, not all "major" faults in the basin appear to have characteristics that appreciably limit groundwater flow across them. Similarly, there is little evidence from either chemistry or water levels indicating that "minor" faults with small offset of similar sediments substantially limit horizontal groundwater flow, at least on a regional scale.

The geochemical data indicate that major faults actually may enhance or cause vertical groundwater flow in some areas of the MRGB. Elevated water temperatures and high Cl and As concentrations in particular often are in close proximity to "major" faults in the basin, especially in the northern part of the basin, the northeastern part of Albuquerque, and the southeastern part of the basin. These elevated concentrations appear to be indicative of groundwater from a deep source that is moving upward to mix with water at shallower depths in the aquifer system. The association of these elevated concentrations with the locations of faults suggests that vertical movement of groundwater could be enhanced in fault zones by increased vertical conductivity resulting from deformation. Elevated Cl and As concentrations also are common in the vicinity of the structural highs near the northern and southern extents of Albuquerque that separate the sub-basins within the MRGB, and near the structural high/constriction that separates the MRGB from the Socorro Basin to the south (Plummer et al. 2004). Upward leakage in this area could account for the elevated Cl and As concentrations.

Summary

Measurements of the chemical and isotopic composition of groundwater from 288 wells and springs in the Middle Rio Grande Basin of central New Mexico were used to refine the conceptual model of groundwater flow in the Upper Santa Fe aquifer system, and to improve understanding of the area's water resources. The extensive regional coverage, supplemented with data from the US Geol Surv NWIS and city of Albuquerque water-quality database, resulted in identification and mapping of the spatial extent of 12 regional sources of water to the basin, and estimation of radiocarbon ages.

The composition of most water in the basin changes little after recharge, and can be traced over large distances through the primarily siliciclastic sediment of the aquifer system. Radiocarbon ages adjusted for geochemical reactions and mixing in the aquifer system are nearly identical to the unadjusted radiocarbon ages and ranged from modern to more than 30 ka.

Predominant sources of water to the basin include (1) recharge from mountains along the north, east and southwest (median age 5–9 ka); (2) seepage from the Rio Grande and Rio Puerco (median age 4–8 ka), and from Abo and Tijeras Arroyos (median age 3–9 ka); (3) inflow of saline water along the southwest basin margin (median age 20.4 ka); and (4) inflow along the northern basin margin (median age 19.9 ka), which probably represents recharge from the Jemez Mountains during the last glacial period.

Piezometer nests provided critical information on variations in chemical and isotopic composition, and radiocarbon age with depth to approximately 600 m below the water table in the vicinity of Albuquerque and several other locations in the northern part of the basin. In some cases, the data from piezometers and other wells permitted characterization of the three-dimensional aspects of water composition, showing that paleo-water (approximately 20 ka), present at the water table through the west-central part of the basin, extends beneath more recent mountain-front recharge in northern parts of the basin, and beneath water of Rio Grande origin under western parts of Albuquerque. Age gradients from two piezometer nests indicate "modern" (past few thousand years) recharge rates of ~3 cm year^{-1} for infiltration from the Rio Grande at Albuquerque and recharge along the eastern mountain front at Albuquerque. Historically, there have been higher amounts of recharge to the Eastern Mountain Front zone at Albuquerque than to vicinities north or south of Albuquerque along the eastern mountain front.

Measurements of the ^{2}H and ^{18}O isotopic composition of source waters to the basin and mapping of the stable isotopic composition of groundwater helped to delineate flow directions and boundaries between hydrochemical zones. The stable isotope data for groundwater in the vicinity of Albuquerque show a relatively sharp transition between recharge from the Sandia Mountains to the east and infiltration of paleo Rio Grande water.

The geochemical data show that groundwater flowing along the axis of a groundwater trough in the west-central part of the MRGB originated in the area of the Jemez Mountains during the last glacial period. Although hydraulic heads indicate that water sourced at the western margin of the basin and at the Rio Grande should be flowing into the trough, the geochemical data indicate that, over the past ~10 ka, these waters have not yet reached the center of the trough. The absence of water sourced from the Rio Grande and from the western margin near the axis of groundwater trough indicates that the trough is a transient rather than a long-term feature of the aquifer system.

The $\delta^{13}C$ isotopic composition of dissolved inorganic carbon in groundwater is remarkably constant throughout most of the basin, indicating a nearly constant historical

 DOI 10.1007/s10040-004-0324-6

predominance of C_4 over C_3 plants in recharge areas for the aquifer system, and minimal water–rock reaction following recharge. However, during the past 1 ka, or perhaps even more recently, the $\delta^{13}C$ isotopic composition of dissolved inorganic carbon of water recharged along the basin margins has become depleted in ^{13}C, and may indicate a recent increase in C_3 plant abundance relative to C_4 plants, as has been observed in other parts of the Southwest.

Extensive chemical and isotopic datasets, such as obtained for the MRGB, are uncommon in the hydrologic sciences. This study demonstrates some of the benefits of obtaining a diverse and extensive chemical and isotopic dataset when characterizing hydrochemical processes in groundwater systems, and when there is need to refine the conceptual model of the aquifer system. In the companion papers (Sanford et al. 2004a, 2004b), the radiocarbon ages and delineation of the boundaries between hydrochemical zones from this study are used to help calibrate a groundwater-flow model for the basin.

Acknowledgements The authors thank the numerous individual landowners who provided access to their wells. We thank the governors and staff of the Pueblos of Cochiti, Isleta, Jemez, Sandia, San Felipe, Santa Ana, Santo Domingo, and Zia for permitting us to sample wells, and assisting in locating wells and records of well construction. The authors also thank Bill White with the Bureau of Indian Affairs for his assistance in contacting the Pueblos and his advice about the most appropriate wells for sampling. Water samples from many of the windmills on Pueblo lands could not have been obtained without the generous assistance of John Sanchez and the windmill crew of the Southern Pueblos Agency.

Individuals from the US Forest Service, the Bureau of Land Management, the US Fish and Wildlife Service, Kirtland Air Force Base, Sandia National Laboratories, the New Mexico Office of the State Engineer, the New Mexico Environment Department, the University of New Mexico, the city of Albuquerque, the city of Belen, and the town of Los Lunas provided access to wells and assisted in locating the most appropriate wells for sampling. We thank Doug Earp and others with the city of Albuquerque Environment Department for their assistance. The cooperation of Rio Rancho Utilities, Rio Grande Utilities, Sandia Peak Utility Company, National Utilities, New Mexico Utilities, DRESCO, Intel, AT&T, King Brothers Ranch, and the Huning Ltd. Partnership in providing access to wells is gratefully acknowledged.

We thank our colleagues with the US Geol Surv, Jerry Casile, Mike Doughten, Julian Wayland, Peggy Widman, Andrew Stack, Anne Burton, Brian C. Norton, David Jones, Ami Mitchell, Daniel Webster, Tyler Coplen, Kinga Revesz, Robert L. Michel, Fred Gebhardt, R.K. DeWees, Jim Bartolino, Joe Sterling, Carolina Trevizo, and Lori Shue for assistance in field sampling, laboratory analysis, assistance in locating wells, data processing, drafting of illustrations, and manuscript preparation.

Finally, the authors would like to thank Doug McAda, Mark Hudson, and Scott Minor of the US Geol Surv, Fred Phillips of New Mexico Institute of Mining and Technology, and John Hawley and Sean Connell of the New Mexico Bureau of Geology and Mineral Resources (NMBGMR) who shared their knowledge and advice about the hydrology and geology of the basin. The manuscript was improved appreciably at several stages of preparation by the constructive reviews of US Geol Surv colleagues Jim Bartolino, Don Thorstenson, Tom Reilly, Pierre Glynn, John Izbicki, and an anonymous reviewer. This work was supported by funds from the Ground Water Resources Program and the National Research Program of the US Geological Survey.

References

Anderholm SK (1985) Clay-size fraction and powdered whole-rock X-ray analyses of alluvial-basin deposits in central and southern New Mexico. US Geol Surv Open-File Rep 85-173:18

Anderholm SK (1988) Ground-water geochemistry of the Albuquerque–Belen Basin, central New Mexico. US Geol Surv Water-Resources Investigations Rep 86-4094:110

Anderholm SK (1997) Water-quality assessment of the Rio Grande valley, Colorado, New Mexico, and Texas — shallow groundwater quality and land use in the Albuquerque area, central New Mexico 1993. US Geol Surv Water-Resources Investigations Rep 97-4067:73

Anderholm SK (2001) Mountain-front recharge along the east side of the Albuquerque Basin, central New Mexico (revised). US Geol Surv Water-Resources Investigations Rep 00-4010:36

Bard E, Hamelin B, Fairbanks R, Zindler A (1990) Calibration of the ^{14}C timescale over the past 30,000 yr using mass spectrometric U–Th ages from Barbados corals. Nature 345:405–410

Bard E, Arnold M, Fairbanks RG, Hamelin B (1993) ^{230}Th–^{234}U and ^{14}C ages obtained by mass spectrometry on corals. Radiocarbon 35:191–199

Bard E, Arnold M, Hamelin B, Tisnerat-Laborde N, Cabioch G (1998) Radiocarbon calibration by means of mass spectrometric $^{230}Th/^{234}U$ and ^{14}C ages of corals: an updated database including samples from Barbados, Mururoa and Tahiti. Radiocarbon 40:1085–1092

Bartlein PJ, Edwards ME, Shafer SL, Barker ED Jr (1995) Calibration of radiocarbon ages and the interpretation of paleoenvironmental records. Quaternary Res 44:417–424

Bartolino JR, Cole JC (2002) Ground-water resources of the Middle Rio Grande Basin, New Mexico. US Geol Surv, Circular 1222:132

Bartolino JR, Niswonger RG, III (1999) Numerical simulation of vertical ground-water flux of the Rio Grande from groundwater temperature profiles, central New Mexico. US Geol Surv Water-Resources Investigations Rep 99-4212:34

Bexfield LM, Anderholm SK (1997) Water-quality assessment of the Rio Grande Valley, New Mexico, and Texas — groundwater quality in the Rio Grande flood plain, Cochiti Lake, New Mexico, to El Paso, Texas 1995. US Geol Surv Water-Resources Investigations Rep 96-4249:93

Bexfield LM, Anderholm SK (2000) Predevelopment water-level map of the Santa Fe Group aquifer system in the Middle Rio Grande Basin between Cochiti Lake and San Acacia, New Mexico. US Geol Surv Water-Resources Investigations Rep 00-4249:1sheet

Bexfield LM, Anderholm SK (2002) Spatial patterns and temporal variability in water quality from City of Albuquerque supply wells and piezometer nests, with implications for the groundwater flow system. US Geol Surv Water-Resources Investigations Rep 01-4244:101

Bexfield LM, Lindberg WE, Anderholm SK (1999) Summary of water-quality data for City of Albuquerque drinking-water supply wells 1988–97. US Geol Surv Open-File Rep 99-195: 138

Bjorklund LJ, Maxwell BW (1961) Availability of ground water in the Albuquerque area, Bernalillo and Sandoval Counties, New Mexico. New Mexico State Engineer Tech Rep 21:117

Boutton TW, Archer SR, Midwood AJ, Zitzer SF, Bol R (1998) $\delta^{13}C$ values of soil organic carbon and their use in documenting vegetation change in a subtropical savanna ecosystem. Geoderma 82:5–41

Connell SD (2001) Stratigraphy of the Albuquerque Basin, Rio Grande Rift, central New Mexico: a progress report. In: Connell SD, Lucas SG, Love DW (eds) Stratigraphy and tectonic development of the Albuquerque Basin, central Rio Grande Rift. New Mexico Bureau of Mines and Mineral Resources Open-File Report 454B, Socorro, NM, pp A1-A27

Connell SD, Allen BD, Hawley JW (1998) Subsurface stratigraphy of the Santa Fe Group from borehole geophysical logs, Albuquerque area, New Mexico. New Mexico Geology 17:79–87

 DOI 10.1007/s10040-004-0324-6

Connin SL, Betancourt J, Quade J (1998) Late Pleistocene C_4 plant dominance and summer rainfall in the southwestern United States from isotopic study of herbivore teeth. Quaternary Res 50:179–193

Constantz J, Thomas CL (1996) The use of streambed temperature profiles to estimate the depth, duration, and rate of percolation beneath arroyos. Water Resour Res 32:3597–3602

Epstein HE, Lauenroth WK, Burke IC, Coffin DP (1997) Productivity patterns of C_3 and C_4 functional types in the US Great Plains. Ecology 78:722–731

Flint AF, Flint LE, Kwicklis EM, Fabryka-Martin JT, Bodvarsson GS (2002) Estimating recharge at Yucca Mountain, Nevada, USA: comparison of methods. Hydrogeol J 10:180–204

Grauch VJS, Gillespie CL, Keller GR (1999) Discussion of new gravity maps for the Albuquerque Basin area. In: Pazzaglia FJ, Lucas SG (eds) Albuquerque geology. New Mexico Geological Society Fiftieth Annual Field Conference, 22–25 September 1999. New Mexico Geological Society, pp 119–124

Grauch VJS, Sawyer DA, Keller GR, Gillespie CL (2001) Contributions of gravity and aeromagnetic studies to improving the understanding of subsurface hydrogeology, Middle Rio Grande Basin, New Mexico. In: Cole JC (ed) US geological survey middle Rio Grande Basin study. Proceedings of the fourth annual workshop, Albuquerque, New Mexico, 15–16 February 2000, US Geol Surv Open-File Rep 00-488:3–4

Grover HD, Musick HB (1990) Shrubland encroachment in southern New Mexico, USA: an analysis of desertification processes in the American southwest. Climatic Change 17:305–330

Haneberg WC, Hawley JW (eds) (1996) Characterization of hydrogeologic units in the Northern Albuquerque Basin, New Mexico. In: Hawley JW, Haneberg WC, Whitworth TM (compilers) Hydrogeologic investigations in the Albuquerque Basin, central New Mexico 1992–1995. New Mexico Bureau of Mines and Mineral Resources Open-File Report 402, Socorro, NM, section 402C

Hawley JW (1996a) Hydrologic setting of the Albuquerque Basin area. In: Hawley JW, Haneberg WC, Whitworth TM (compilers) Hydrogeologic investigations in the Albuquerque Basin, central New Mexico 1992–1995. New Mexico Bureau of Mines and Mineral Resources Open-File Report 402, Socorro, NM, section 402B

Hawley JW (1996b) Hydrogeologic framework of potential recharge areas in the Albuquerque Basin, central Valencia County, New Mexico. In: Hawley JW, Whitworth TM (eds) Hydrogeology of potential recharge areas for the basin- and valley-fill aquifer systems, and hydrogeochemical modelling of proposed artificial recharge of the upper Santa Fe aquifer, northern Albuquerque Basin, New Mexico. New Mexico Bureau of Geology and Mineral Resources Open-File Report 402-D, 608 pp

Hawley JW, Haase CS (1992) Hydrogeologic framework of the northern Albuquerque Basin. Open-File Report 387:74 New Mexico Bureau of Mines and Mineral Resources, Socorro, NM

Hawley JW, Haase CS, Lozinsky RP (1995) An underground view of the Albuquerque Basin. In: Ortega-Klett CT (ed) The water future of Albuquerque and the Middle Rio Grande Basin. Proceedings of the 29th Annual New Mexico Water Conference, 3–4 November 1994. New Mexico Water Resources Research Institute WRRI Report No 290, Las Cruces, NM, pp 34–55

Helsel DR, Hirsch RM (1995) Statistical methods in water resources. Elsevier Science BV, New York

Heywood CE (1992) Isostatic residual gravity anomalies of New Mexico. US Geol Surv Water-Resources Investigations Rep 91-4065:27

Huang Y, Street-Perrott FA, Metcalf SE, Brenner M, Moreland M, Freeman KH (2001) Climate change as the dominant control on glacial–interglacial variations in C_3 and C_4 plant abundance. Science 293:1647–1651

Kalin RM (2000) Radiocarbon dating of groundwater systems. In: Cook PG, Herczeg AL (eds) Environmental tracers in subsurface hydrology. Kluwer, Dordrecht, pp 111–144

Kelley VC (1977) Geology of Albuquerque Basin, New Mexico. New Mexico Bureau of Mines and Mineral Resources Memoir 33, Socorro, NM

Kernodle JM (1998) Simulation of ground-water flow in the Albuquerque Basin, central New Mexico, 1901–95, with projections to 2020. US Geol Surv Open-File Rep 96-209:54

Kernodle JM, Miller RS, Scott WB (1987) Three-dimensional model simulation of transient ground-water flow in the Albuquerque–Belen Basin, New Mexico. US Geol Surv Water-Resources Investigations Rep 86-4194:58

Kernodle JM, McAda DP, Thorn CR (1995) Simulation of groundwater flow in the Albuquerque Basin, central New Mexico 1901–1994, with projections to 2020. US Geol Surv Water-Resources Investigations Rep 94-4251:114

Kitagawa H, van der Plicht J (1998a) Atmospheric radiocarbon calibration to 45,000 yr B.P.: Late glacial fluctuations and cosmogenic isotope production. Science 279:1187–1190

Kitagawa H, van der Plicht J (1998b) A 40,000-year varve chronology from Lake Suigetsu, Japan: extension of the ^{14}C calibration curve. Radiocarbon 40:505–515

Kitagawa H, van der Plicht J (2000) Atmospheric radiocarbon calibration beyond 11,900 cal BP from Lake Suigetsu laminated sediments. Radiocarbon 42:369–380

Liu B, Phillips FM, Campbell AR (1996) Stable carbon and oxygen isotopes in pedogenic carbonates, Ajo Mountains, southern Arizona: implications for paleoenvironmental change. Palaeogeogr Palaeoclimatol Palaeoecol 124:233–246

Logan LM (1990) Geochemistry of the Albuquerque municipal area, Albuquerque, New Mexico. MSc Thesis, New Mexico Institute of Mining and Technology, Socorro, NM

Lozinsky RP (1988) Stratigraphy, sedimentology, and sand petrology of the Santa Fe Group and pre-Santa Fe Tertiary deposits in the Albuquerque Basin, central New Mexico. New Mexico Institute of Mining and Technology, PhD Thesis, Socorro, NM

McAda DP (1996) Plan of study to quantify the hydrologic relations between the Rio Grande and the Santa Fe Group aquifer system near Albuquerque, central New Mexico. US Geol Surv Water-Resources Investigations Rep 96-4006:58

McAda DP, Barroll P (2002) Simulation of ground-water flow in the Middle Rio Grande Basin between Cochiti and San Acacia, New Mexico. US Geol Surv Water-Resources Investigations Rep 02-4200:81

McPherson GR, Boutton TW, Midwood AJ (1993) Stable carbon isotope analysis of soil organic matter illustrates vegetation change at the grassland/woodland boundary in southeastern Arizona, USA. Oecologia 93:95–101

Minor SA, Shock NA (1998) Characterizing faults in the Middle Rio Grande Basin: results from the Cochiti and Santo Domingo Pueblos. US Geol Surv Open-File Rep 98-337:22–23

Monger HC, Cole DR, Gish JW, Giordano TH (1998) Stable carbon and oxygen isotopes in Quaternary soil carbonates as indicators of ecogeomorphic changes in the northern Chihuahuan Desert, USA. Geoderma 82:137–172

Moore D (1999) Precipitation chemistry data on the Sevileta National Wildlife Refuge, 1989–1995: Sevilleta LTER Database, accessed March 2, 1999, at http://sevilleta.unm.edu/research/local/nutrient/precipitation/#data

Mozley PS, Goodwin LB (1995) Patterns of cementation along a Cenozoic normal fault — a record of paleoflow orientations. Geology 23:539–542

Mozley P, Beckner J, Whitworth TM (1995) Spatial distribution of calcite cement in the Santa Fe Group, Albuquerque Basin, NM — implications for ground-water resources. New Mexico Geol 17:88–93

Phillips FM, Tansey MK, Peeters LA (1989) An isotopic investigation of groundwater in the central San Juan Basin, New Mexico: carbon-14 dating as a basis for numerical flow modeling. Water Resour Res 25:2259–2273

 DOI 10.1007/s10040-004-0324-6

Plummer LN, Bexfield LM, Anderholm SK, Sanford WE (2001) Geochemical characterization of ground-water flow in the Santa Fe Group aquifer system, Middle Rio Grande Basin, New Mexico. In: Cole JC (ed) US Geological Survey Middle Rio Grande Basin Study. Proceedings of the Fourth Annual Workshop, Albuquerque, New Mexico, 15–16 February 2000. US Geol Surv Open-File Rep 00-488:7–10

Plummer LN, Bexfield LM, Anderholm SK, Sanford WE, Busenberg E (2004) Geochemical characterization of ground-water flow in the Santa Fe Group aquifer system, Middle Rio Grande Basin, New Mexico. US Geol Surv Water-Resources Investigations Rep 03-4131:395 (in press)

Plummer LN, Prestemon EC, Parkhurst DL (1994) An interactive code (NETPATH) for modeling NET geochemical reactions along a Flow PATH. Version 2.0. US Geol Surv Water-Resources Investigations Rep 94-4169:130

Reeder HO, Bjorklund LJ, Dinwiddie GA (1967) Quantitative analysis of water resources in the Albuquerque area, New Mexico? Computed effects on the Rio Grande of pumpage of ground water, 1960–2000. New Mexico State Engineer Technical Report 33:34

Russell LR, Snelson S (1990) Structural style and tectonic evolution of the Albuquerque Basin segment of the Rio Grande Rift. In: Pinet B, Bois C (eds) The potential of deep seismic profiling for hydrocarbon exploration. Proc French Petroleum Inst Res Conf, Editions Technip, Paris, pp 175–207

Sanford WE, Plummer LN, Bexfield LM (1998) Using environmental tracer data to improve the US Geological Survey MODFLOW model of the Middle Rio Grande Basin. In: US Geological Survey Middle Rio Grande Basin Study: Second Annual Workshop, Albuquerque, New Mexico, Feb. 1998. US Geol Surv Open-File Rep 98-337:13–14

Sanford WE, Plummer LN, McAda DP, Bexfield LM, Anderholm SK (2001) Estimation of hydrologic parameters for the groundwater model of the Middle Rio Grande Basin using carbon-14 and water-level data. In: Cole JC (ed) US Geological Survey Middle Rio Grande Basin Study. Proceedings of the Fourth Annual Workshop, Albuquerque, New Mexico, 15–16 February 2000. US Geol Surv Open-File Rep 00-488:4–6

Sanford WE, Plummer LN, McAda DP, Bexfield LM, Anderholm SK (2004a) Use of environmental tracers to estimate parameters for a predevelopment-ground-water-flow model of the Middle Rio Grande Basin, New Mexico. US Geol Surv Water-Resources Investigations Rep. 03-4286 (in press)

Sanford WE, Plummer LN, McAda DP, Bexfield LM, Anderholm SK (2004b) Hydrochemical tracers in the Middle Rio Grande Basin, USA: 2. Calibration of a groundwater model. Hydrogeol J DOI: s10040-004-0326-4 (this volume)

Scanlon BR, Healy RW, Cook PG (2002) Choosing appropriate techniques for quantifying groundwater recharge. Hydrogeol J 10:18–39

Stone BD, Allen BD, Mikolas M, Hawley JW, Haneberg WC, Johnson PS, Allred B, Thorn CR (1998) Preliminary lithostratigraphy, interpreted geophysical logs, and hydrogeologic characteristics of the 98th Street core hole, Albuquerque, New Mexico. US Geol Surv Open-File Rep 98-210:82

Stuiver M, Reimer PJ (1993) Extended ^{14}C data base and revised CALIB 3.0 ^{14}C age calibration program. Radiocarbon 8:534–540

Stuiver M, Kromer B, Becker B, Ferguson CW (1986) Radiocarbon age calibration back to 13,300 years B.P. and the ^{14}C age matching of the German oak and US bristlecone pine chronologies. Radiocarbon 28:980–021

Stuiver M, Reimer PJ, Bard E, Beck JW, Burr GS, Hughen KA, Kromer B, McCormac G, van der Plicht J, Spurk M (1998) INTCAL98 radiocarbon age calibration, 24,000–0 cal B.P. Radiocarbon 40:1041–1083

Thomas CL (1995) Infiltration and quality of water for two arroyo channels, Albuquerque, New Mexico 1988–92. US Geol Surv Water-Resources Investigations Rep 95-4070:63

Thorn CR, McAda DP, Kernodle JM (1993) Geohydrologic framework and hydrologic conditions in the Albuquerque Basin, central New Mexico. US Geol Surv Water-Resources Investigations Rep 93-4149:106

Tiedeman CR, Kernodle JM, McAda DP (1998) Application of nonlinear-regression methods to a ground-water flow model of the Albuquerque Basin, New Mexico. US Geol Surv Water-Resources Investigations Rep 98-4172:90

Titus FB (1961) Ground-water geology of the Rio Grande trough in north-central New Mexico, *with sections* on the Jemez Caldera and Lucero Uplift. In: Northrop SA (ed.) Guidebook of the Albuquerque country. New Mexico Geological Society, 12th Field Conference, pp 186–192

Titus FB (1963) Geology and ground-water conditions in eastern Valencia County, New Mexico. New Mexico Bureau of Mines and Mineral Resources Ground-Water Report 7, Socorro, NM

Wigley TML, Plummer LN, Pearson FJ Jr (1978) Mass transfer and carbon isotope evolution in natural water systems. Geochim Cosmochim Acta 42:1117–1139

Wigley TML, Plummer LN, Pearons FJ Jr (1979) Errata. Geochim Cosmochim Acta 43:1395

Yapp CJ (1985) D/H variations of meteoric waters in Albuquerque, New Mexico, USA. J Hydrol 76:63–84

Zhu C, Winterle JR, Love EI (2003) Late Pleistocene and Holocene groundwater recharge from the chloride mass balance method and chlorine-36 data. Water Resour Res (39)7:1182, DOI: 10.1029/2003WR001987